DEVELOPING LUMINESCENT NANOPROBES FOR LABELING FOCAL ADHESION COMPLEX PROTEINS AND PERFORMING COMBINED AFM-TIRF IMAGING OF THESE CONJUGATES

A Thesis

by

BHAVIK NATHWANI

Submitted to the Office of Graduate Studies of
Texas A&M University
in partial fulfillment of the requirements for the degree of

MASTER OF SCIENCE

May 2008

Major Subject: Biomedical Engineering

DEVELOPING LUMINESCENT NANOPROBES FOR LABELING FOCAL ADHESION COMPLEX PROTEINS AND PERFORMING COMBINED AFM-TIRF IMAGING OF THESE CONJUGATES

A Thesis

by

BHAVIK NATHWANI

Submitted to the Office of Graduate Studies of
Texas A&M University
in partial fulfillment of the requirements for the degree of

MASTER OF SCIENCE

Approved by:

Chair of Committee,	Kenith E. Meissner
Committee Members,	Anshu B. Mathur
	Alvin T. Yeh
	David C. Zawieja
Head of Department,	Gerald L. Cote

May 2008

Major Subject: Biomedical Engineering

ABSTRACT

Developing Luminescent Nanoprobes for Labeling Focal Adhesion Complex Proteins and Performing Combined AFM-TIRF Imaging of These Conjugates.

(May 2008)

Bhavik Nathwani, B.E, Saurashtra University

Chair of Advisory Committee: Dr. Kenith E. Meissner

Recent progress in the field of semiconductor nanocrystals or Quantum Dots (QDs) has seen them find wider acceptance as a tool in biomedical research labs. As produced, high quality QDs synthesized by high temperature organometallic synthesis, are coated with a hydrophobic ligand. Therefore, they must be further processed to be soluble in water and made biocompatible.

A process to coat the QDs with silk fibroin, a fibrous protein derived from the *Bombyx mori* silk worm, is described. Following the coating process, the characterization of size, optical properties and biocompatibility profile of these particle systems is described. In addition, conjugation of the silk fibroin coated QDs to different labeling proteins such as phalloidin and streptavidin is described.

Proteins on the surface of ovarian cancer cells (HeyA8) and of cytoskeletal components participating in the formation of focal adhesion complex (FAC), such as F-actin in endothelial cells (HUVECS) were labeled using the bio-conjugated QDs.

Various imaging techniques such as epi-fluorescence, TIRF and AFM were used to study the QD labeled cells. Overall the project has produced luminescent nanoprobes that enable the study of FAC formation dynamics and potentially a better in vivo fluorescent marker tool.

DEDICATION

I dedicate this work to my loving family: my parents for having initiated me on the academic path and my loving siblings and wife for their constant encouragement.

ACKNOWLEDGEMENTS

I would like to express my appreciation of my master's thesis advisor, Dr. Kenith E. Meissner for his guidance and support. He was a constant source of encouragement and a "guide" in the true sense of the word.

I would also like to acknowledge the important role played by Dr Anshu B. Mathur throughout my work on this project. The excellent facilities at her lab and the insightful discussions that we had played a very important role in shaping this work.

I would also like to thank them both for providing the financial assistance necessary for this work.

I would also like to thank Dr Alvin yeh for his class on Tissue Engineering and his encouragement as a committee member.

I would also like to thank Dr Dave Zawieja for the discussions that we had and for his encouragement as a committee member.

I would like to acknowledge Dr Zhiping Luo and Dr Ken Dunner's help in acquiring TEM images.

Special mention needs to be made of the tremendous help that I received from Mona Jaffari, Clark Needham and Kyle Borque. Without their help, it would have been impossible to produce the many samples that were needed all through the work. I would also like to acknowledge Carmen Rios's contribution. She initiated my interest in exploring the use of silk fibroin. I would also like to acknowledge Chintan Trivedi's

support. His encouraging words played an important role to see me through some difficult times.

I would also like to thank my wife, Nidhi Nathwani, for her love, support and encouragement. I would also like to thank her for all that she has put up with while I have unabashedly been working on this project neglecting all my other responsibilities.

TABLE OF CONTENTS

LIST OF FIGURES

FIGURE Page

FIGURE Page

LIST OF TABLES

CHAPTER I

INTRODUCTION AND MOTIVATION

Semiconductor nanocrystals or Quantum Dots (QDs) have rapidly gained popularity as a fluorescent tool in biomedical/biology labs (The terms semiconductor nanocrystals and QDs are used interchangeably throughout the text). Favorable properties such as size tunable absorption/emission, improved photostability and narrow emission peak to enable spectral multiplexing contribute towards their popularity.[1-4] In addition to ex vivo labeling, QDs have recently also been used for in vivo applications.[5, 6] Significant progress has been made in fabricating monodisperse QDs,[7] while a variety of coating chemistries have been developed to make these particles both water soluble and biocompatible.[8, 9] Current techniques to solubilize the QDs rely on

1. Ligand exchange using thiols[2, 10]
2. Ligand exchange using oligomeric phosphines,[11] dendrons,[12] and peptides[13]
3. Encapsulation by a layer of amphiphilic diblock or triblock copolymers[5]
4. Encapsulation by silica shells,[3] phospholipid micelles,[1] polymer beads,[14] polymer shells,[15] or amphiphilic polysaccharides[16]
5. Combination of layers of different molecules giving the necessary colloidal stability to qdots[17]

This thesis follows the style of *Nano Letters*.

Procedures to employ ligand exchange using any of the above mentioned primers are easy to implement, however, the bond holding the primer to the nanocrystal is dynamic, and thus yields relatively low stability to the system in water. Furthermore, during the ligand exchange process there might be slow dissolution of CdSe/ZnS in solution, which limits the applicability of this system for biological applications.[18]

The procedures of encapsulating QDs with polymers have been quite involved.[19] The resultant particles have been successfully used for ex vivo applications. However, their feasibility for use in in vivo applications has been limited by their half-lives in biological systems.[19, 20]

While the use of recombinant proteins to coat the QDs after ligand exchange has been reported earlier,[17, 21] no known literature exists on noncovalently coating the QDs with a natural protein without prior ligand exchange.[17, 21]

This report discusses the fabrication, characterization and application of silk fibroin coated QDs. Silk fibroin is fibrillar protein derived from the *Bombyx mori* silkworm. Furthermore, the conjugation of the SF coated QD particles to different marker proteins using the conventional EDC (1-ethyl-3-(3-dimethylaminopropyl) carbodiimide hydrochloride) chemistry is reported. Additionally, the results of performing AFM-TIRF imaging of cells labeled with this particle/protein system are discussed.

CHAPTER II

BACKGROUND

Quantum Dots (QDs) result from the quantum confinement of electron hole pairs (excitons) in all three spatial dimensions.[22] The first experimental evidence of the existence of such quasi-zero dimensional particles was reported by Ekimov and colleagues.[23] Murray et al published the first report on colloidal synthesis process of fabrication of nearly monodisperse CdX (X-Se, Te, S) QDs.[24] Many researchers have reported adaptations of this technique subsequently.[25-28] Peng and Peng reported a modified route to the synthesis of CdX nanocrystals.[7] Our lab utilized an adaptation of the Peng and Peng approach to synthesize II-VI CdSe semiconductor nanocrystals. The nanocrystals were fabricated using the high temperature organometallic synthesis procedure. Fabrication was carried out at 300^0 C under nitrogen environment.

For surface passivation and to enhance the quantum yield of these particles, an inorganic coating of ZnS shell was epitaxially grown on these dots.[29] The outer surface of the core/shell assembly was covered by trioctylphosphine oxide (TOPO)* used as coordinating ligand during the fabrication reaction. These hydrophobic TOPO ligands made the QDs insoluble in solvents such as water, which in turn also rendered them bio-incompatible.

As discussed in the previous section, various techniques have been proposed to circumvent the issues of water solubility and biocompatibility of QDs. QDs coated with different synthetic polymers have gained popularity for in-vitro[30] and ex vivo labeling[31]

but have been less successful for in vivo applications due to their half-lives in biological systems.[20, 32]

To alleviate these issues, it was decided to coat QDs with a natural protein. The choice of a natural protein, silk fibroin (SF), was guided by the desirable properties of SF. Some of these properties such as oxygen and water permeability, relatively low thrombogenecity, low inflammatory response, protease susceptibility, and high tensile strength with flexibility directly influence the applicability of these particles for in vivo studies.[33-35] The structure of SF consists of a light chain and a heavy chain linked by a single disulfide bond. The light chain is approximately 25 kDa and the heavy chain is approximately 325 kDa in mass.[36] A sericin coating binds the two chains together. Removal of this sericin coating is necessary to lower the thrombogenecity and inflammatory response of SF.[35] Use of SF to coat nanoparticles for drug delivery and the evaluation of it's performance in vivo has been reported earlier.[33] Since biocompatibility is necessarily a surface phenomenon, it was natural for us to speculate a similar biocompatibility profile for QDs coated with SF.

Thus, there were two major scientific goals, that dictated the need for the development of such particles:

1. Need for QDs with better applicability for in vivo studies.

2. Need for a tool to label focal adhesion complex (FAC) proteins.

2.1 FAC Background

Cells produce extracellular matrix (ECM), organize it, and degrade it. Through matrix receptors, transmembrane proteins, this matrix is tied to the intracellular

components of the cells. It is believed that this matrix not only provides mechanical support to the cells but also plays a significant role in mechano-transduction of signals from the extra-cellular environment to the inside of the cell. This ECM signaling plays an important role in coordinating cell growth and development.[37] Furthermore, it contributes towards cell behavior in response to perturbation in homeostasis.[38] Recent developments also suggest the role of matrix receptors in cancer progression and potential therapeutic approaches exploiting this role.[39-41]

Although several types of molecules are studied as matrix receptors, integrins are the most widely studied. Furthermore, one of the most intensely researched modes of integrin signaling comes through the study of focal adhesions.[42] Focal adhesions are the anchorage points of the plasma membrane of a cell on the substratum over which it is moving.[43] At the point of adhesion, integrins cluster and provide anchorage to the cell. When integrins cluster, focal adhesion kinase (FAK) is recruited by intracellular anchor proteins such as talin or paxillin. The clustered FAK molecules in turn cross phosphorylate and create docking sites for a variety of other intracellular signaling proteins such as vincullin, creating a link between the extracellular matrix and the cytoskeleton. Integrin mediated adhesions can undergo dynamic changes transforming from dot-like focal complexes to stress fiber associated focal contacts and maturing to form fibronectin bound fibrillar adhesions.[44] Intracellular anchorage to the adhesion is provided by actin fibers. Figure 1 shows a schematic of a focal adhesion complex.

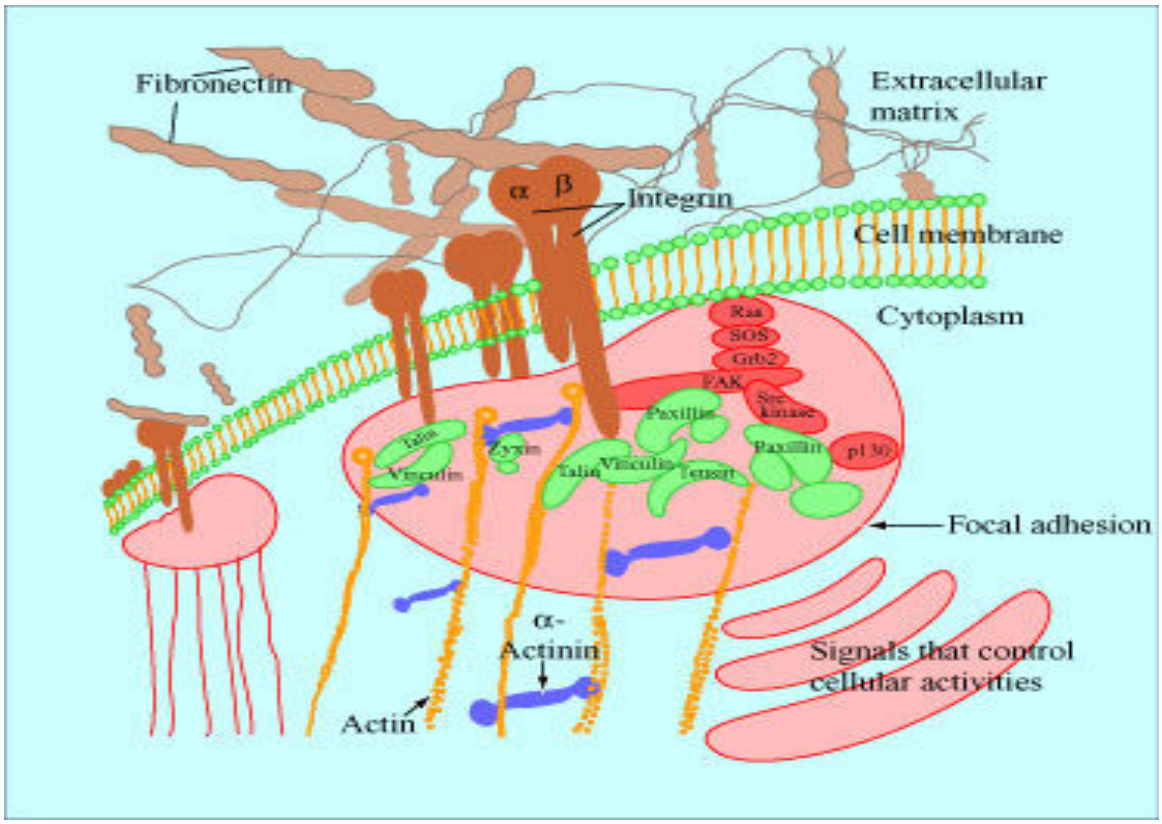

Figure 1. Sketch showing the focal adhesion complex (FAC) formed at the cell-matrix interface[42].

Although the statics of the formation of integrin-mediated adhesions have been studied in detail earlier,[45] recent development suggests that an important role is played by other proteoglycans, such as syndecans, in the adhesion formation dynamics and the signaling pathways associated.[46-48] Of special interest is the role of adhesion dynamics in designing engineered tissue scaffolds[49] and in designing better drug delivery vehicles.[50]

The current scenario dictates development of an imaging tool that enables the study of cell adhesion dynamics. In response to these issues, this thesis describes the development of a luminescent nanoprobe that would enable the study of cell adhesion dynamics. Also presented are images demonstrating the labeling of endothelial cells with these nanoprobes. Fluorescence imaging of cells labeled with these particles was

performed along with TIRF and AFM imaging. The following sections will explain in detail the advantages of using these imaging tools over traditional epi-fluorescence imaging.

2.2 Total Internal Reflection Fluorescence Microscopy (TIRF)

Different mechanisms are often employed in fluorescence microscopy to restrict the area of a specimen excited by a light source. This type of restriction often results in an improved signal-to-noise ratio, which translates into a better spatial resolution. Total Internal Reflection Fluorescence microscopy (TIRF) utilizes evanescent waves to illuminate a limited specimen region (approx 100 nm) immediately adjacent to the interface between two media having different refractive indices.

2.3 Principle of Evanescent Wave Generation

The schematic in figure 2 shows the principle of "evanescent waves" that governs TIRF systems:

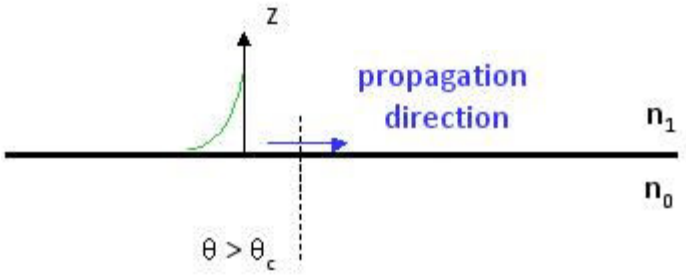

Figure 2. Schematic illustrating the principle of generation of "evanescent waves" at the interface of materials with different refractive indices.

Snell's law gives the relationship between angles of incidence and refraction for light impinging on the interface of two media with different refractive indices. The following equation describes the Snell's law:

$$n_1 \sin\theta_1 = n_2 \sin\theta_2$$

where n_1 and n_2 are refractive indices of the two media, and θ_1 and θ_2 are angles of incidence and refraction respectively.

When light traveling through a medium of high refractive index is incident on an interface with a low refractive index material on the other side, at an incidence angle θc, such that the refracted light makes an angle of 90^0 with the normal, this angle is known as the critical angle and is given by,

$$\theta_c = \sin^{-1}(n_2/n_1)$$

If the light is incident at an angle greater than the critical angle the light gets "Totally Internally Reflected" (TIR) and no refracted wave is produced. Furthermore, at the interface a standing wave or an "evanescent field" propagates through the low refractive index material. The frequency of the evanescent field is the same as that of the incident light and the intensity of the evanescent field exponentially "decays" with distance.

The intensity of the evanescent field decreases exponentially with distance and is given by:

$$I(z) = I_0 e^{-z/d}$$

where,

$$d = \frac{\lambda_0}{4\pi}\left[n_1^2 \sin^2\theta - n_2^2\right]^{-1/2}$$

where, I(z) is the intensity of the evanescent wave at a height, z, above the interface, I_0 is the initial intensity, λ_0 is the wavelength of the incident light, and d is the distance travelled by the evanescent field from the interface.

TIRF has been used to visualize cell-substrate interface.[51-53] Furthermore, since the evanescent field illuminates a small distance into the cell, avoiding the unwanted fluorescence acquired from the rest of the cell, studies have shown a substantial improvement in the signal-to-noise ratio while imaging cell-substrate contacts using TIRF imaging over epi fluorescence imaging.[54] TIRF has also been used to study individual components of the FAC such as the actin filaments.[55] Other applications of TIRF studied so far include:

1. visualization and spectroscopy of single molecule fluorescence near a surface[54, 56-60]

2. tracking of secretory granules in intact cells before and during the secretory process[61, 62]

3. measurements of the kinetic rates of binding of extracellular and intracellular proteins to cell surface receptors and artificial membranes[53, 63]

4. micromorphological structures and dynamics on living cells[64, 65]

5. long term fluorescence movies of cells during development in culture[66]

6. comparison of membrane-proximal ionic transients with simultaneous transients deeper in the cytoplasm[67]

Hence, if we combine the advantages of TIRF system, high signal-to-noise ratio and an ability to excite the FAC (region of interest for the author), with the advantages of QDs, such as ability to spectrally multiplex the information, it would provide a very effective tool to study the dynamics of formation and functioning of a Focal Adhesion Complex (FAC).

2.4 Atomic Force Microscopy

Atomic Force Microscopy (AFM) is a member of the family of Scanning Probe Microcopies (SPM). It measures inter-atomic forces between the AFM cantilever and the surface while spatially scanning the surface.[68] In its simplest form an AFM works by scanning, raster scan, the surface of interest with a tiny tip mounted at the end of a cantilever. A piezoelectric actuator enables sub-angstrom accuracies in the tip-surface separation. The deflection of the cantilever, resulting from its interaction with the surface being scanned, is monitored using a precision laser. The laser beam is reflected from the back surface of the cantilever tip towards a split photodetector, that amplifies the cantilever deflections. A negative feedback loop, connected to the cantilever deflection sensor, keeps the tip surface interaction at a fixed value controlling the tip surface distance. The amount of feedback signal received at each scanning point is used to reconstruct the topography of the surface being scanned.[69]

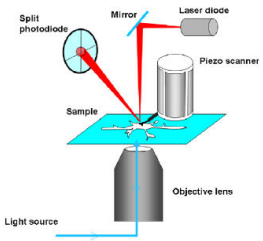

Figure 3. Schematic of an AFM coupled with an inverted microscope[69].

A schematic of the AFM system used for this research is shown in figure 3. Use of AFM for biological imaging and for manipulation of biological macromolecules have been reported earlier. Some of the biological applications have included:

1. Studying the dynamics of cell division for adherent cells[70]
2. Antibody recognition imaging[71]
3. Drug discovery by studying the effect of specific molecules on the cytoskeleton of the cell[72, 73]
4. Unzipping DNA molecules[74] and bacterial surface layers[75]
5. Study of protein mechanics[76]
6. Study the statics of focal adhesion complex (FAC) formation[77]

Recent studies have used combined AFM-TIRF approach to study cellular mechanics.[65, 78] A similar approach is reported in this thesis, describing the use of AFM-TIRF microscopy to image QD labeled FAC proteins. An AFM tip can be used in tapping mode to induce formation of FAC and the TIRF system can simultaneously be used to image the dynamics of this formation. Previous studies reporting the use of QDs

as fluorophores to carry out combined AFM-TIRF imaging have relied on labeling the AFM tip with QDs.[79] As reported in the study, the approach results in a very sensitive nano-ruler based on fluorescence and can be used to study processes such as protein unfolding. The technique described in this thesis modifies this approach to label the FAC proteins and study the formation of FAC, induced by AFM tip, using TIRF signal.

CHAPTER III

MATERIALS AND METHODS

3.1 Fabrication of QDs

High quality monodisperse CdSe/ZnS QDs were prepared using an adaptation of a method previously described in literature.[7] The target amounts of all chemicals used are given in table I. cadmium oxide (CdO, Alfa Aesar – 99.998%), tetradecyl phosphonic acid (TDPA, Alfa Aesar – 98%) and trioctyl phosphine oxide (TOPO, Sigma Aldrich – 99%) were taken in a 3-neck flask and were heated to 340^0 C for 1 hour under constant Ar flow (approx 1ml/s). The heating was carried out in a metal bath containing an alloy of bismuth with a melting point of 110^0 C. The temperature of the metal bath was measured using a type-K thermocouple in a stainless steel sheath, providing feedback to a (Omega CSC32) benchtop controller. This step was used to reduce CdO to Cd^{2+}. The presence of TDPA allowed the binding of Cd^{2+} to the coordinating solvent, TOPO in our case.

A shot of TOP:Se (trioctyl phosphine, Sigma Aldrich 90% : selenium powder, Sigma Aldrich 99.99%) was prepared because it is easier, safer and more convenient to handle as compared to Se powder. The molar concentration of Se used to prepare this shot was 30% more than that of Cd^{2+}. This exhausts all the Cd^{2+} during the fabrication process reducing the chances of background noise signal from Cd photoluminescence. The Se shot was prepared in a round bottom flask with a resealing cap that permitted Ar purging of the flask. The purging prevents oxidation of the TOP. The solution was

stirred using a teflon coated magnetic stirrer for 1 hour, allowing the selenium to dissolve in the TOP.

Table 1. Amounts of each chemical used in the fabrication of one standard batch of CdSe quantum dots.

Chemical:	TOP	Se	CdO	TDPA	TOPO
Amount:	2.4 ml	0.0411 g	0.0514 g	0.0566 g	3.7768 g

Table 2. Amounts of each chemical used in growing a ZnS shell over a standard batch of CdSe quantum dots.

Chemical:	TOP	Dimethyl Zinc	Hexamethyldisilathiane
Amount:	6.3 ml	1.6 ml	0.42 ml

The temperature of the Cd^{2+} containing flask was lowered to 300^0 C. The TOP:Se precursor (generally 2.6 ml) was aspirated out from the round bottom flask using a 12 inch, 18-gauge stainless steel needle and was injected very slowly in the Cd containing flask.

The reaction was allowed to continue for 7 min. The reaction time governs the size of the particles and by implication the photoluminescence emission peak wavelength of the particles. At this point, the CdSe QD cores are ready. But to improve the photoluminescence quantum yield of the nanocrystals and to achieve surface passivation of the QD surface, the QD cores are overcoated with ZnS to form a core/shell QD.

A ZnS precursor was prepared using dimethyl zinc (DMZ, Sigma Aldrich – 1 M in Heptane), and hexamethyldisilathian (HMDS, Sigma Aldrich) and using TOP as a

solvent. Again, like TOP:Se the ZnS precursor was prepared in a round bottom flask with a resealing cap to allow purging of the flask with Ar. The ZnS precursor was allowed to react for 2 hours before using it to coat CdSe QDs.

Immediately following the CdSe core synthesis, the temperature of the reaction pot (CdSe QDs) was reduced to 200 C. ZnS precursor was injected into this pot very slowly (approx. 3ml/min) using a 12 inch, 18-gauge needle. To ensure the growth of a thin layer of ZnS, the ZnS was allowed to grow for 30 min. Afterwards, the temperature of the flask was reduced to 100^0 C. This allowed the annealing of the core/shell QDs.

Samples of QDs were then quenched in Methanol (EMD). A glass eye dropper was used to aliquot the samples out of the reaction pot (0.8+/-0.2 ml) in 10+/-2 ml methanol. The high QD to methanol ratio would ensure immediate quenching of the reaction. These samples were cleaned repeatedly with methanol to remove excess unreacted TOPO. To carry out the cleaning process the samples were repeatedly centrifuged out of methanol and re-suspended again in methanol. After 4 cleaning cycles, the sample were re-dispersed in chloroform (Sigma Aldrich) for storage. A photograph of the experimental setup used to carry out the entire synthesis process is shown in figure 4.

Figure 4. Experimental set up to fabricate quantum dots.

3.2 Water Solubility of QDs

Figure 5 is the schematic of an average CdSe/ZnS/TOPO QD made in the lab:

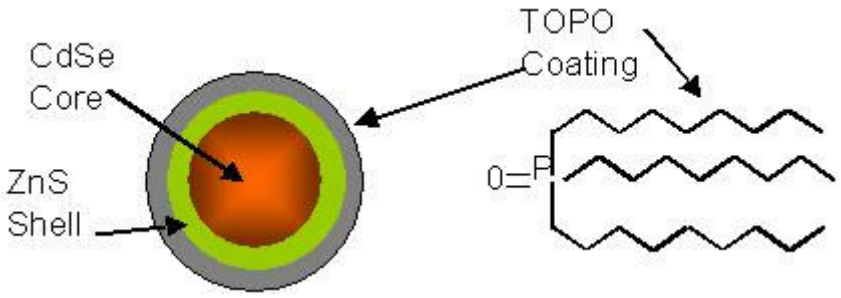

Figure 5. Schematic of CdSe/ZnS/TOPO QD.

To make these particles water soluble, an additional coating is required. Initially, we coated them with polyethyleneimine (PEI). Figure 6 shows the chemical structure of PEI and figure 7 is a schematic showing the coating of TOPO coated QDs with PEI.

—NH—[CH2]2—

Figure 6. Structure of polyethyleneimine (PEI).

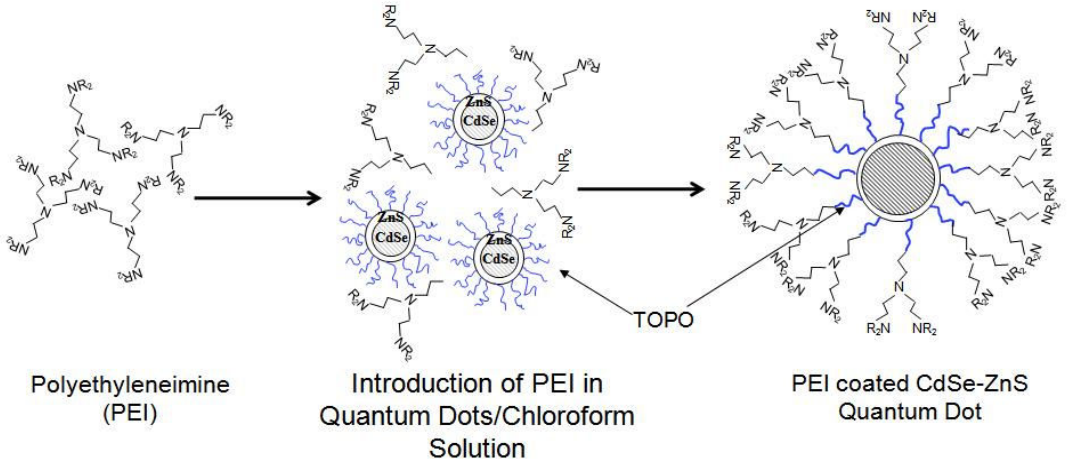

Figure 7. Schematic showing the coating of CdSe/ZnS QDs by PEI.

3.3 PEI Coating of QDs

Earlier reported technique[8] to coat QDs with PEI was modified for use in our lab. 10 ml of cleaned CdSe/ZnS/TOPO was alliquoted in a scintiallation vial using a micro-pipette (OD=0.1). 1 mg of PEI (polyethyleneimine, Sigma Aldrich 408727) was added to the vial. The mixture was vortexed and allowed to react for 10 min. The solvent from the vial was then vacuum dried. The thin coating left on the inner wall of the vial at the end of the drying process was re-dispersed in DI water. The PEI coating was achieved and the QDs became soluble in water.

There were 2 original goals that the coating process was designed to achieve:

1. Make the QDs water soluble

2. Make them biocompatible

Examination of the sample demonstrates that the PEI coated QDs were water soluble.

3.4 Cell Cultures

To test the biocompatibility of PEI coated QDs, HeyA8 ovarian cancer cells were cultured using RPMI 1640 media with 10% FBS and 1% gentamycin. The cells were cultured in T75 flasks. The concentration of the cultured cells was $1x10^6$ per flask. The cell vial was taken out of liquid nitrogen and incubated to 37^0 C in a water bath. 1 ml of cells were transferred from the vial to a 10 ml conical flask containing 9 ml media. The cells were then centrifuged out of the media. The conical flask was placed in a centrifuge at 4^0 C and centrifuged at 200 g. After centrifugation thee supernatant was aspirated out of the flask and the cells were resuspended in 10 ml media. The media containing the cells was then transferred to T75 flasks and the flask was placed in the incubator. The entire process was carried out aseptically inside a biological safety cabinet. The media was changed every 2 days. When the cultured cells reached confluence, they were exposed to PEI coated QDs. 3 ml of QD/PEI (OD=0.1 cm^{-1}) was used per flask. The cells were exposed to the QDs for 1 hour. At the end of 1 hour, the QDs were aspirated out of the flask and the flask was given 3 PBS washes. 10 ml of media was then added to the flask.

3.5 Silk Fibroin Coating of QDs

The silk fibroin coating of QDs was carried out in three steps.

3.5.1 Degumming Silk

Raw silk for this project was kindly donated by Dr. S. Hudson (TECS, North Carolina State University, Raleigh, NC). As mentioned in the introduction section, the raw silk has a sericin coating, which must be removed to reduce the thrombogenecity of the silk. The removal of sericin coating is known as the "degumming process". 0.25% w/v sodium dodecylsulfate (Sigma Aldrich) and 0.25% w/v sodium carbonate (Sigma Aldrich) were dissolved in ultra-pure water. This soap solution was then placed in a glass beaker on a magnetic stirrer and brought to 100^0 C. Raw silk was added at 1:100 w/v. The mixture was heated for 1 hour. The alkaline soap solution was then drained and the degummed silk was heated to 100^0 C in distilled water for an additional hour to wash the surfactant from the silk. Finally, remaining sericin and surfactants were removed completely by rinsing the silk under running distilled water. The washed silk was then air dried and stored.[80]

3.5.2 Coating of QDs with Degummed Silk

0.1% w/v solution of degummed silk fibroin was prepared in chloroform and the solution was then sonicated. Samples were prepared with 1, 2, 3 and 4 hours sonicated silk fibroin in chloroform. It is speculated that the beta sheet structure of silk fibroin gets broken into a random coil structure during the sonication process. Sonicated silk fibroin (SF) solution was then added to QDs (absorbance = 0.1 cm^{-1}) in chloroform. 50% v/v solution was prepared. This solution was further sonicated for 5 min to achieve

homogeneity. The coating of QDs by SF was almost instantaneous. A schematic of the coating process is shown in figure 8.

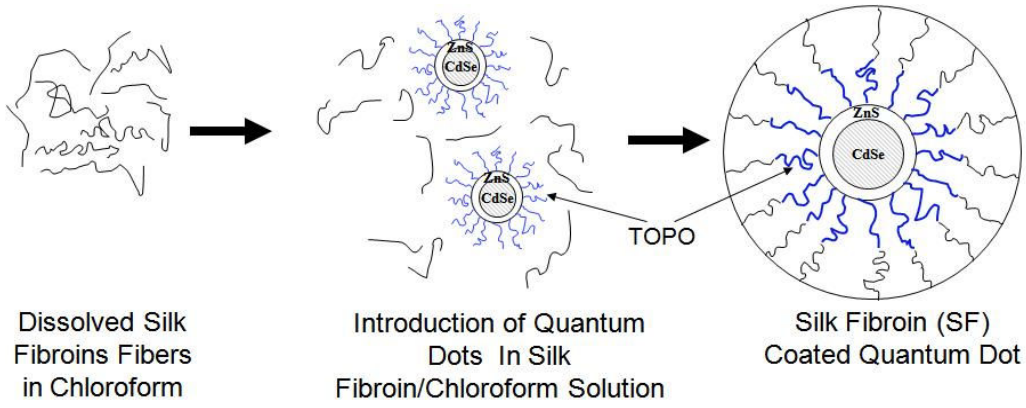

Figure 8. Schematic showing the encapsulation of CdSe/ZnS QDs by SF.

3.5.3 Crystallization of SF Coated QDs

The solvent from the SF coated QDs was vacuum dried. A thin layer of SF coated QDs was left on the walls of the vial. 50% v/v methanol (MeOH) and DI water was added to the vial. The amount of this solution was just enough to cover the QD layer (approx 1 ml). The solution was gently mixed. The solvent from the resultant solution was heated off at 70^0 C. A layer of crystallized SF coated QDs was left behind on the inner walls of the vial. This was re-dispersed in 10 ml DI water. The solution was sonicated for 10 min to achieve homogeneity and re-dispersion of QDs in water.

3.6 Characterization of SF Coated QDs

3.6.1 Optical Characterization of SF Coated QDs

The photoluminescence (PL) spectra of uncoated QDs and SF coated QDs were recorded using quantamaster fluorometer (Photon Technologies International – PTI); a fluoremeter, designed to detect the fluorescence or photoluminescence from a sample, is equipped with a wide spectrum light source that is filtered through a monochromator that adjusts the wavelength of the excitation light allowed to pass through to the sample to excite it. The setup of the equipment is given as a part of the appendix. For standard PL characterization, an excitation wavelength of 465 nm was used with a 5 nm excitation slit and an integration time of 1s, while the emission was monitored from 500 to 700 nm with a 1 nm emission slit.

3.6.2 Photoluminescence Quantum Yield

Photoluminescence Quanutm Yield (PLQY) measurements were carried out by comparing the ratio of integrated PL counts of QDs/SF to that of rhodamine 6G (reference). The PLQY of R6G is known to be 95.5% ± 2%. The excitation wavelength used was 500 nm, the peak emission wavelength was 555 ± 10 nm, absorbance at the excitation wavelength 0.05 ± 0.02 cm^{-1} and the length of the sample 1 cm (std glass cuvette – 1 cm wide).

3.6 3 Size Distribution

Transmission electron microscopy (TEM) was performed using a JEOL JEM – 1010 microscope. The crystallized SF coated QDs appeared monodisperse with a size range of 10-14 nm. To corroborate this result, Atomic Force Microscopy (AFM) was performed on these particles using Veeco scientific's Bioscope II.

3.6.4 Cell Cultures

To test the biocompatibility of SF coated QDs the same procedure as was used with PEI coated QDs was followed. HeyA8 ovarian cancer cells were cultured using RPMI 1640 media with 10% FBS and 1% gentamycin. When the cultured cells reached confluence, they were exposed to SF coated QDs. 3 ml of QD/SF (concentration=0.1 cm^{-1}) was used per flask. The cells were exposed to the QDs for 1 hour. At the end of 1 hour, the QDs were aspirated out of the flask and the flask was given 3 PBS washes. 10 ml of media was then added to the flask.

3.6.5 Protein Conjugation

To label the different cell components with a high degree of specificity, there was a need to conjugate QDs/SF with labeling proteins. Samples of SF coated QDs conjugated to streptavidin and phalloidin were prepared.[81]

3.7 QD/Streptavidin Conjugation

Modified EDC chemistry was used to prepare QD streptavidin conjugates. The procedure was modified from that given along with the product kit by Pierce (See appendix). 1 mg EDC (approx 2mM) was mixed with 1.1 mg of sulfo-NHS (approx 5 mM) in a glass vial. The mixture was vortexed to ensure homogeneity. 1 ml of streptavidin was added to the mixture and the reaction allowed to progress for 15 min at room temperature. 1.4 microliter of 2-mercaptoethanol was added to quench this reaction. The mixture was vortexed again to ensure homogeneous quenching of the reaction. SF coated QDs were added to this vial. The QDs were allowed to react with the activated streptavidin for 2 hours. After 2 hours, the reaction was quenched by adding

10mM Hydroxylamine. The mixture was then centrifuged using centrifuge filter tubes to remove any unused reactants from the mixture. The supernatant was collected in a separate vial.

3.8 QD/Phalloidin Conjugation

Modified EDC chemistry was used to prepare QD phalloidin conjugates. 1 mg EDC (approx 2mM) was mixed with 1.1 mg of sulfo-NHS (approx 5 mM) in a glass vial. The mixture was vortexed to ensure homogeneity. 1 ml of phalloidin was added to the mixture and the reaction allowed to progress for 15 min at room temperature. 1.4 microliter of 2-Mercaptoethanol was added to quench this reaction. The mixture was vortexed again to ensure homogeneous quenching of the reaction. SF coated QDs were added to this vial. The QDs were allowed to react with the activated phalloidin for 2 hours. After 2 hours, the reaction was quenched by adding 10 mM Hydroxylamine. The mixture was then centrifuged using centrifuge filter tubes to remove any unused reactants from the mixture. The supernatant was collected in a separate vial.

3.9 Labeling of Cell Surface Proteins Using QD/Streptavidin Conjugates

In order to label the cell surface proteins with QD/streptavidin conjugates, the cell surface proteins were biotinylated using a standard biotinylation kit (Pierce Biotech, 89881). The following was the procedure followed to biotinylate HeyA8 Cells:[82]

1. Media was aspirated from the flask containing the cells.
2. The cells were given 3 PBS washes using ice-cold PBS (pH = 8) to remove all the amine containing media and proteins from the cells.

3. The cells were then trypsinized, 5 ml of trypsin per flask, and allowed to detach from the flask surface for 5 min.

4. The trypsin was neutralized using PBS and the cells were suspended in PBS at a concentration of $25x10^6$.

5. 1 mg of sulfo-NHS-Biotin per ml of cells was added. The approximate concentration of the resulting biotin reagent was 2 mM.

6. The reaction was then allowed to continue at room temperature for 30 min.

7. The cells were then transferred to a glass cover slip.

8. After 1 hour, the cells were given 3 PBS + 10 mM glycine washes to quench and remove excess biotin reagent and byproducts.

9. The flask was then exposed to 3 ml of QD/streptavidin (OD = 0.1).

10. After 1 hour of exposure, the cells were washed with PBS (3x) and media was added to them.

3.10 Labeling of F-actin Using QD/phalloidin Conjugates

In order to label F-actin inside the Human Umbilical Vein Endothelial Cells (HUVECS), the cells were fixed, permeabilized and then exposed to QD/phalloidin. The following steps describe the method used to achieve this:

1. The media was removed from the slide on which HUVECS were grown earlier.

2. 1 ml of 3.7% formaldehyde was added to the slide. Formaldehyde had been pre-heated to 37^0 C.

3. The cells were incubated with 3.7% formaldehyde at room temperature for 10 min.

4. Formaldehyde was then aspirated out and 3 PBS washes were given to the cells.

5. 1 ml of 90% methanol was added per slide. Methanol had been pre-cooled to -20^0 C.

6. The cells were then incubated at room temperature for 5 min.

7. After the methanol was aspirated, the cells were again given 3 PBS washes.

8. The cells were then exposed to 1 ml of QD/phalloidin (OD = 0.1) per slide and incubated at room temperature for 1 hour.

9. After 1 hour the QDs were aspirated out and the PBS added. The cells were now ready for imaging.

CHAPTER IV

RESULTS

This section will report the results achieved during the project. As mentioned in the materials and methods section, CdSe quantum dots were fabricated and were coated with ZnS to improve the quantum yield of the particles. Figure 9 demonstrates this phenomenon.

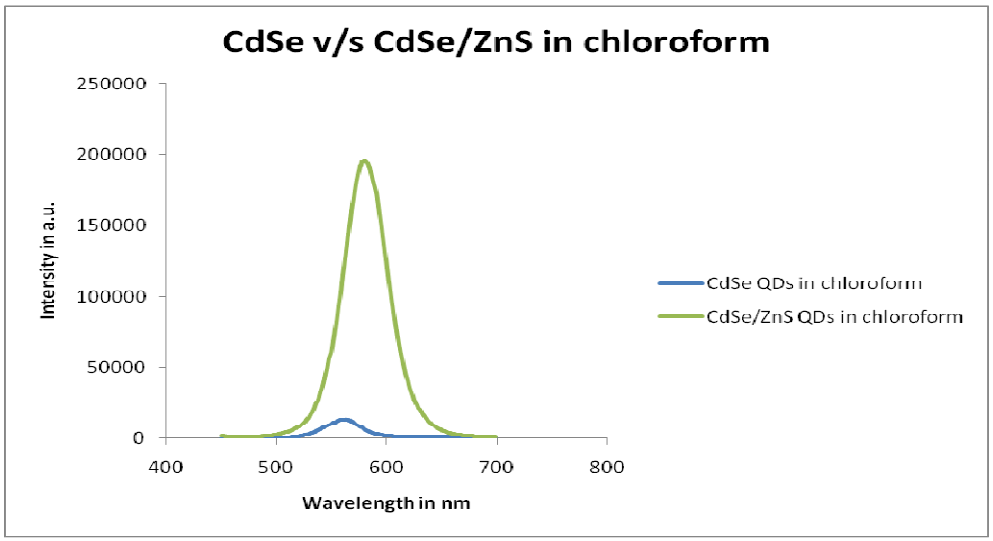

Figure 9. Emission curve for CdSe vs CdSe/ZnS QDs in chloroform.

The luminescence intensity is plotted for absorbance matched samples and the improvement in intensity is better than an order of magnitude (14.4358 times). This value is comparable to the values reported in the literature[83]. Samples with emission peaks ranging from 545 – 610 nm were prepared for various studies. The FWHM of samples varied from approximately 30-40 nm. The higher FWHM curves corresponded

to longer reaction times and implicitly longer emission peak wavelength. "Ostwald ripening"[24] is responsible for the widening of the FWHM. Once the reactants are used up in the reaction pot, the higher energy of smaller nanocrystals promotes their dissolution and this dissolved material gets deposited on larger nanocrystals. This results in a greater inhomogeneity in the size distribution of the sample and consequently a broadening of the emission spectra. This broadening of the emission spectra is also known as "inhomogeneous broadening".

To make the QDs water soluble, the QDs were coated with PEI. Figure 10 shows the emission curve for a representative sample of PEI coated CdSe/ZnS QDs. The quantum yield of QDs was decreased to 90% of original as a result of PEI coating. The pH of PEI coated QDs was acidic (approx 5.5). The pH of the solution was neutralized by adding appropriate amount of NaOH.

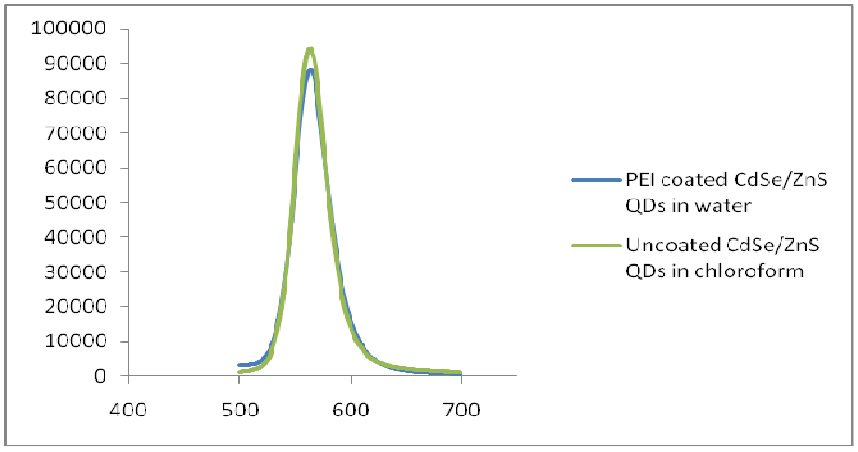

Figure 10. Emission curves for absorption matched CdSe/ZnS QDs in chloroform and PEI coated CdSe/ZnS QDs in water.

HeyA8 cells were cultured and exposed to the PEI coated QDs as described in the materials and methods section. The sample was excited using a 488 nm light source. The QDs emitted at 580 nm. The cells were imaged 1 hour post exposure. Zeiss Axio Observer microscope was used to image the cells. As shown in figure 11 below almost all the cells died within 1 hour post exposure.

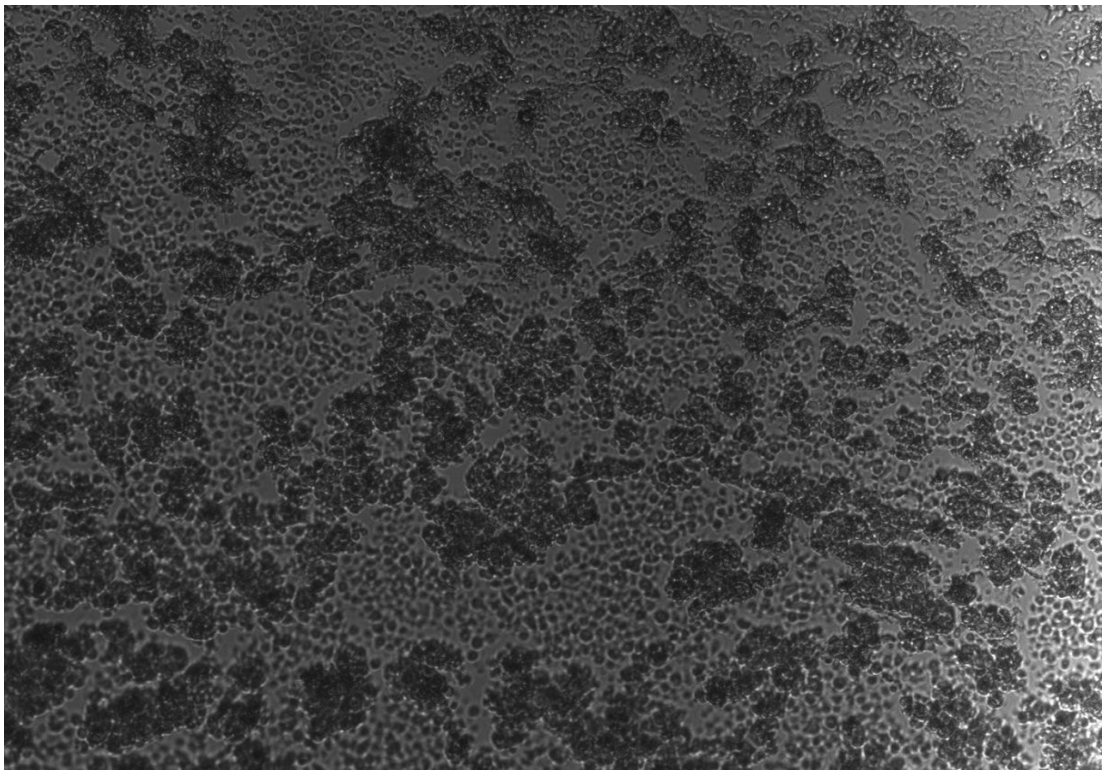

Figure 11. Fluorescence image of HeyA8 cells exposed to PEI coated CdSe/ZnS QDs. Image taken at t=1 hr post exposure.

We speculate that since the PEI is positively charged, the aggregation of these particles inside the slightly negatively charged plasma membrane lead to this toxic effect. As a result of this negative result on preliminary cytotoxicity study, we decided against using PEI for subsequent work. To alleviate the shortcomings of the known coating procedure, a new coating material was needed.

SF was chosen as a coating material due to the many desirable properties[33-35] it has (see Introduction). QDs were then coated with silk fibroin (SF) as described in the experimental section. To characterize these particles TEM and AFM were carried out. Figures 12 and 13 show results of TEM imaging. Figure 12 is a representative of the uncoated QDs. The size of the uncoated CdSe/ZnS QDs in chloroform was found to be 4.378 ± 1.11 nm. Since the uncoated CdSe/ZnS quantum dot was suspended in chloroform, which would dissolve the formvar coating of the copper grid used in the TEM, the solution was diluted using ethanol. Three different dilution factors were used; 1:2, 1:1, and 2:1 ratios of QD/chloroform to ethanol. QDs appeared aggregated in 1:2

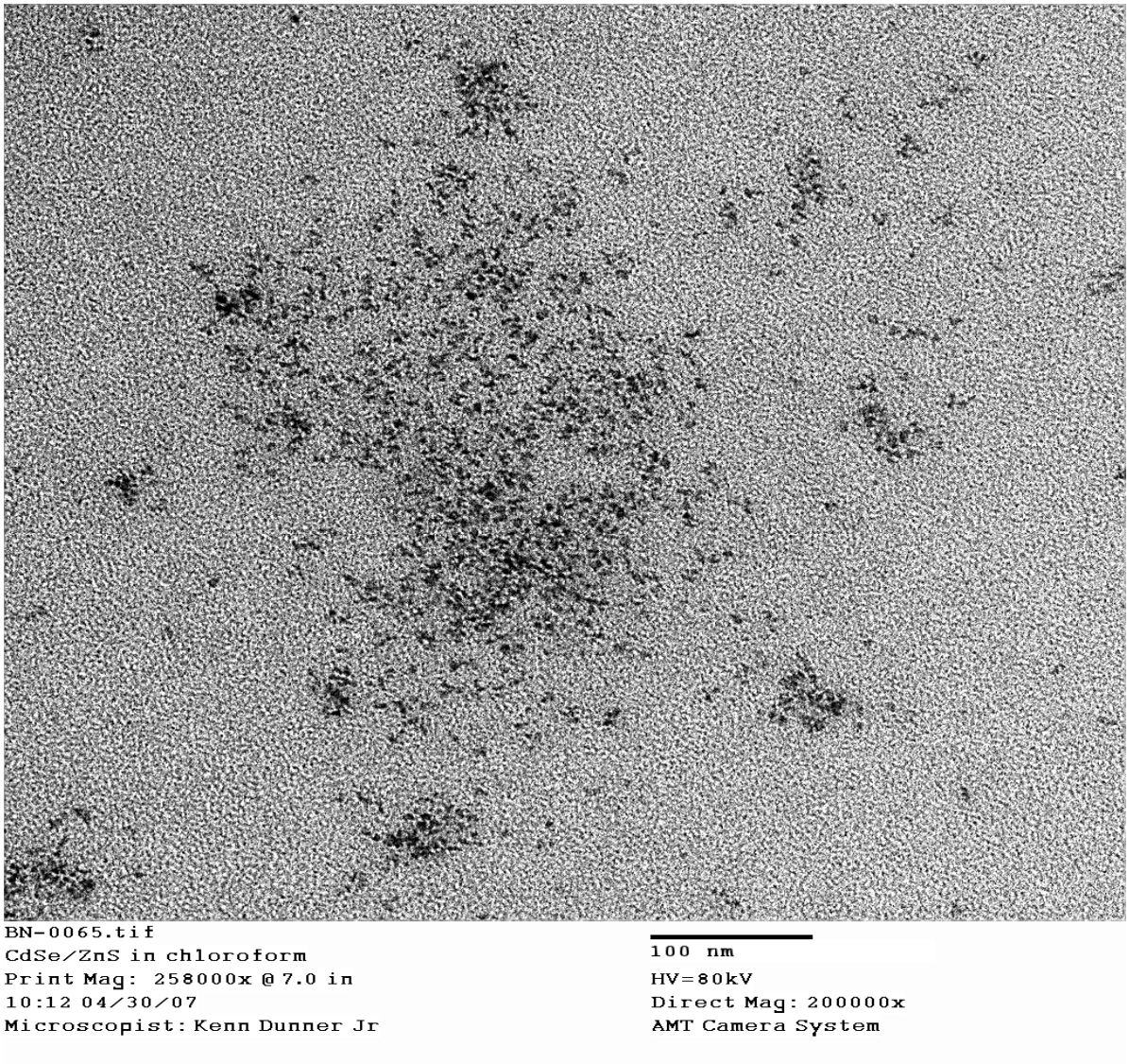

Figure 12. TEM of uncoated CdSe/ZnS QDs in chloroform. Size distribution for these particles was 4.378 ± 1.11 nm. The image corresponds to a 2:1 dilution of QD/chloroform in Ethanol.

and 1:1 dilutions but appeared well distributed in the 2:1 dilution. 20 images per sample were collected with magnifications of 50K, 100K, 200K and 250K. (Dr. Ken Dunner at MDACC and Dr. Zhiping Luo at TAMU helped us get the images.)

Figure 13 shows crystallized silk fibroin coated quantum dots. The size distribution of this sample was found to be 17.59 ± 20.35 nm. The large standard deviation is indicative of polydispersity. Closer examination of the image indicates presence of larger size silk particles that did not coat QDs. To improve the size distribution of SF coated QDs the silk particles needed to be precipitated out of the sample. Size selective precipitation was used to achieve this. Crystallized SF coated sample was transferred to centrifuge tubes (1 ml per tube) using a micro-pipette and was centrifuged at 5000 g for 6 min. Since the non-coating silk fibroin particles were larger in size as compared to the SF coated QDs, they settled at the bottom of the centrifuge tubes. The supernatant was then collected in a separate vial using a micro-pipette.

In figure 14 the size distribution of centrifuged SF coated QDs was 6.65 ± 2.99 nm. The particles were fairly monodisperse as denoted by the standard deviation. A visual inspection of the TEM image confirms this.

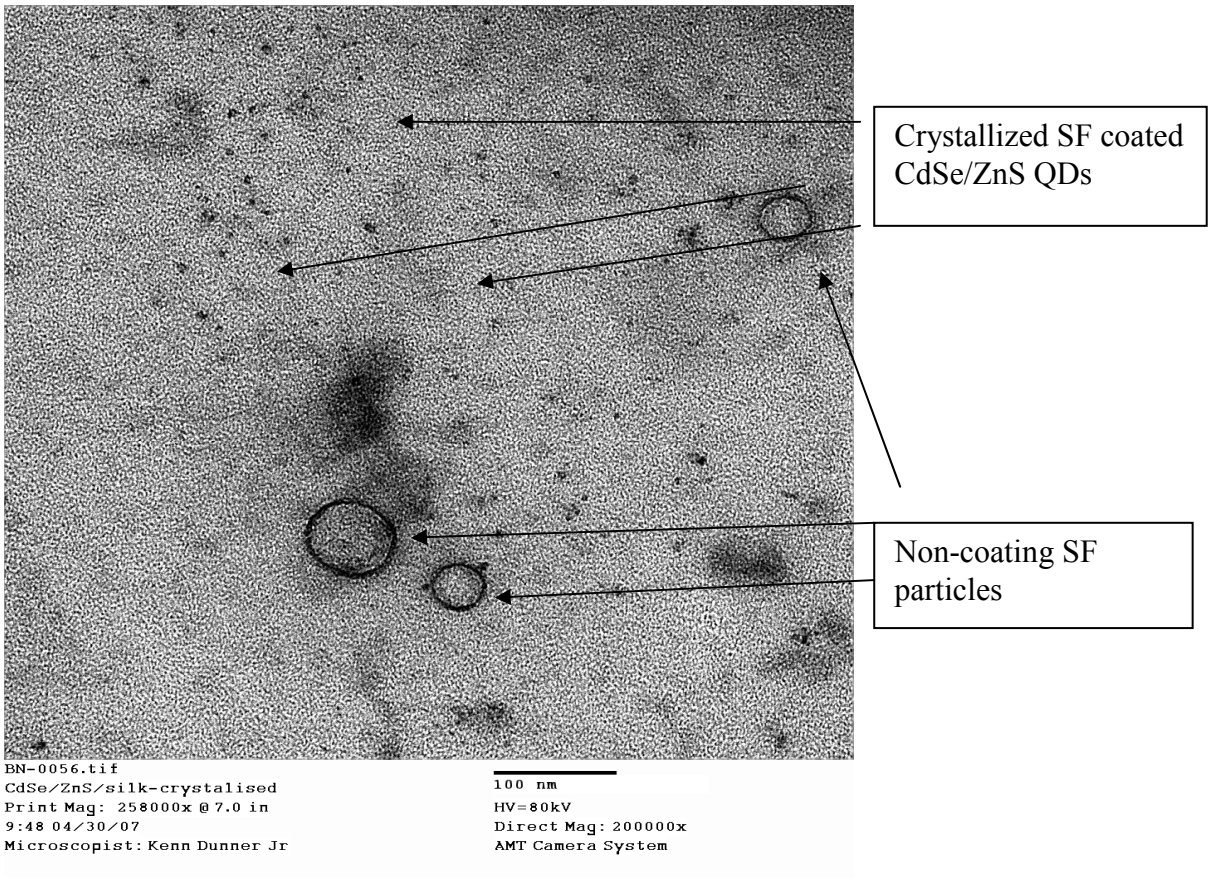

Figure 13. TEM image of crystallized SF coated QDs. Size distribution of these particles was 17.59 ± 20.35 nm. The particles were unprecipitated at this point.

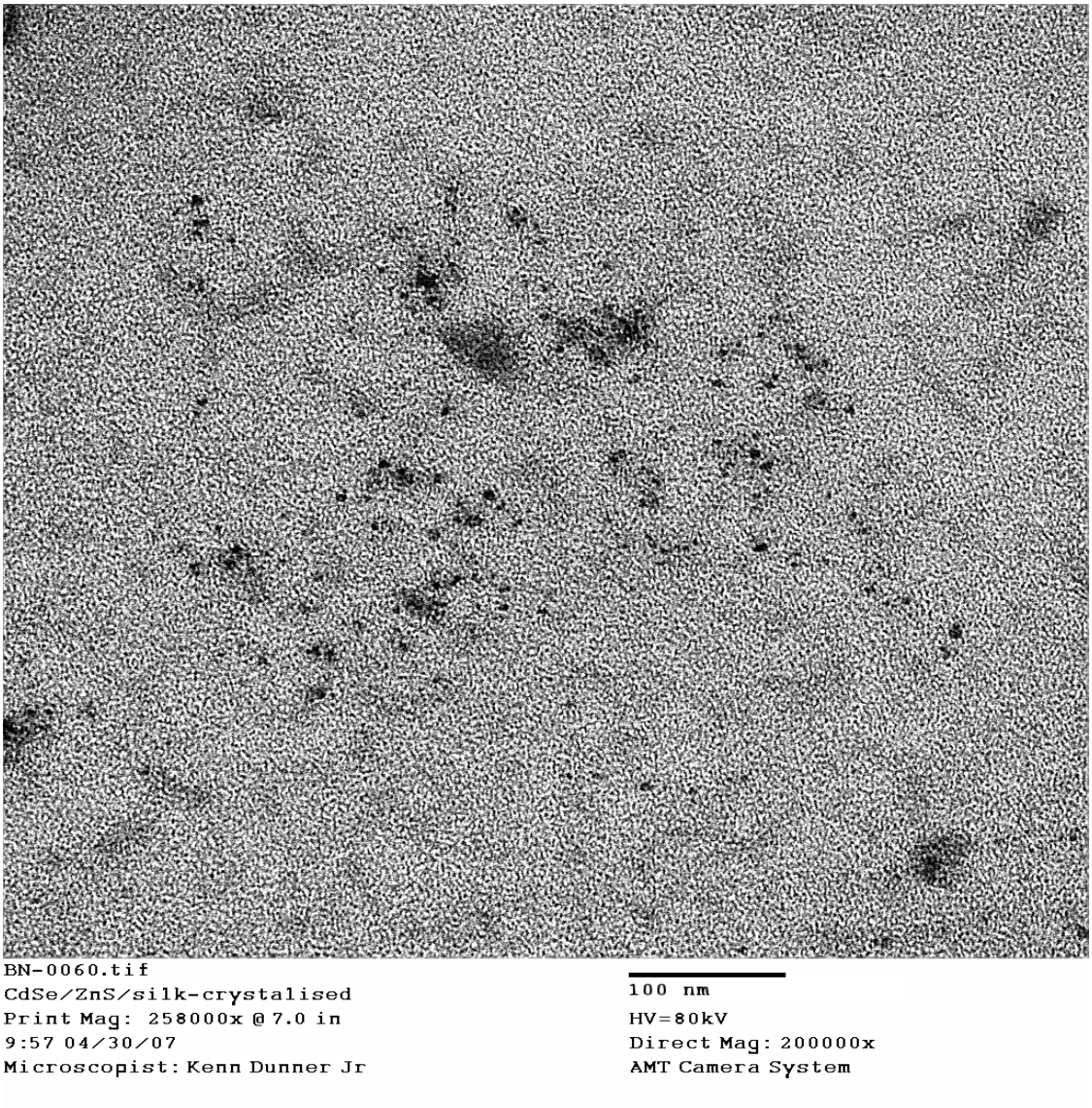

Figure 14. TEM image of crystallized and centrifuged SF coated CdSe/ZnS QDs. Size distribution for this sample was 6.65 ± 2.99 nm.

To corroborate this data AFM was carried out on these samples. Approximately 1 ml of QD sample was transferred from the vial to a microscope cover slip using a micro pipette. A smear of these dots was prepared by sliding a cover slip over the drop of sample. Figures 15 and 16 show AFM results of uncoated and SF coated QDs. The AFM was used in tapping mode air. The coated quantum dots seem to have a preferential axis,

which is aligned with the direction of AFM tip scan. This is indicative of soft coating of the particles. It would be safe to speculate that this would act as an added degree of freedom when the particles are used for in vivo studies as the soft coating will allow for the particles to face lesser steric hindrance while traversing through blood capillaries.

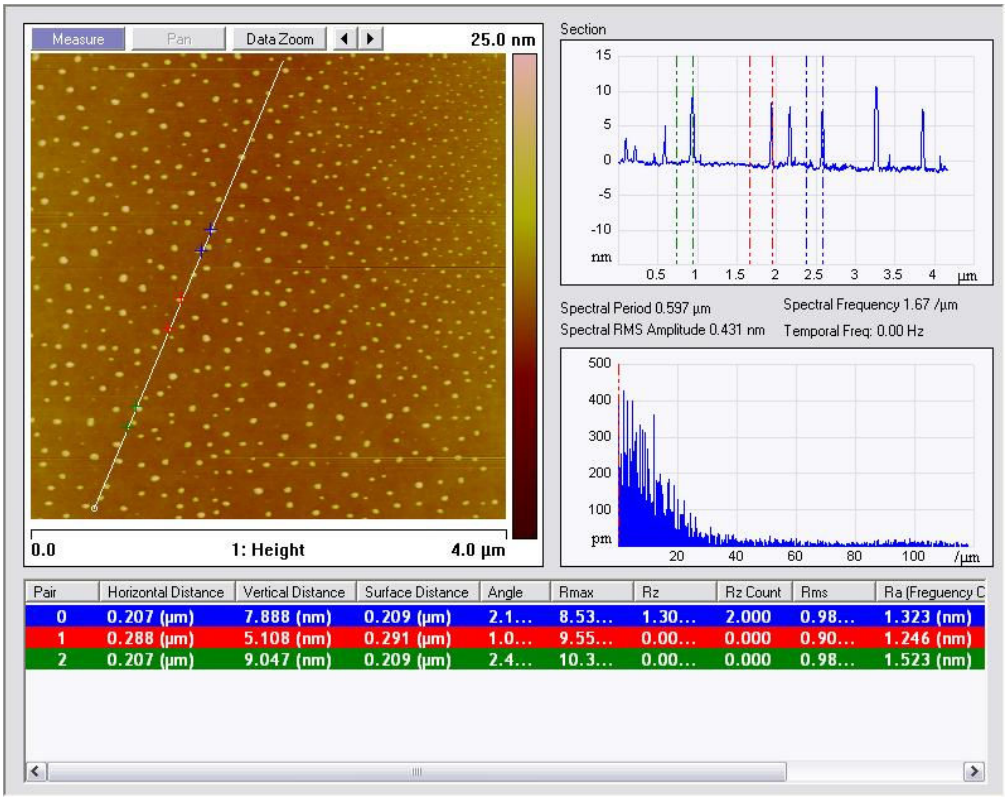

Figure 15. AFM image of uncoated CdSe/ZnS QDs. A smear of the QDs was prepared on a cover slip and scanned using Veeco Scientific's Bioscope II in tapping mode air.

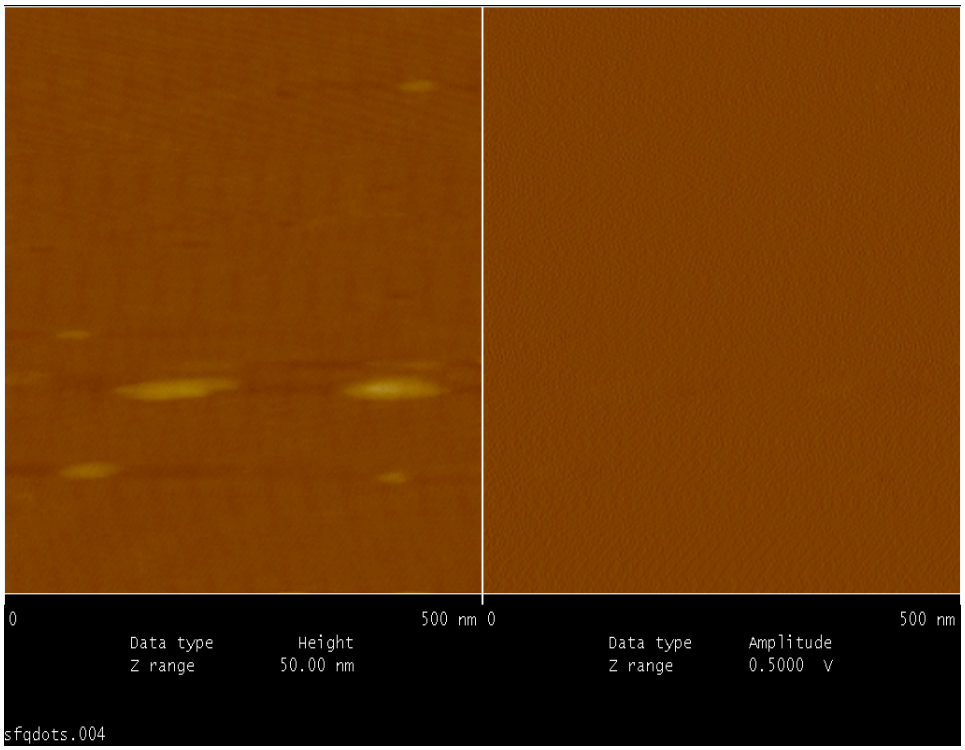

Figure 16. AFM image of crystallized SF coated QDs.

An initial study of the optical properties of SF coated QDs indicated a blue shift in the peak emission wavelength of QDs as shown in figure 17. The amount of shift was a function of the number of hours of SF sonication. Figure 18 shows the blue shift for a 4 hour sonicated sample. The peak emission wavelength shifted by approximately 90 nm to the blue end of the spectrum. Owing to the approximately 2 nm size micro-fibrils[84], resulting from 4 hours of sonication time, consisting of polypeptide chains of gly-ala-gly-ala-gly-ser-gly-ala-ala-gly-tyr[84], we speculated a change in the energy landscape that the exciton experienced.

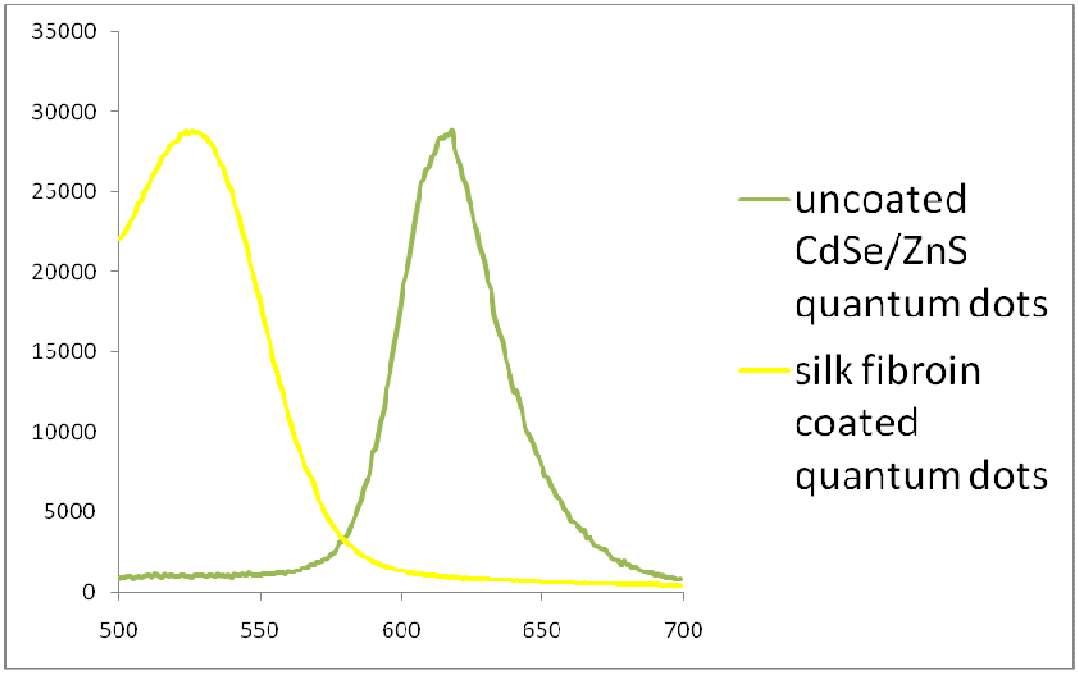

Figure 17. Blue shift of peak emission wavelength of QDs believed to be resulting from SF coating.

A detailed analysis of the particles, however, revealed formation of aggregates of these particles. A representative TEM image is given in Figure 18 demonstrating this observation. To rectify this situation a procedure was developed to crystallize these samples as was described in the experimental section. Post crystallization, size selective precipitation was carried out. Figure 19 is the emission curve of the crystallized SF coated QDs. The curve corresponds to a sample prepared by 4 hours of sonication.

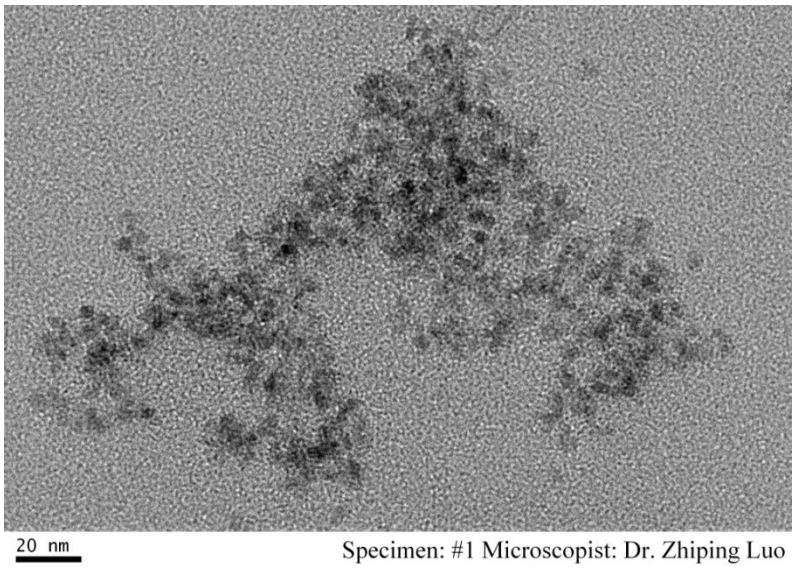

Figure 18. TEM image of aggregated uncrystallized SF coated QDs.

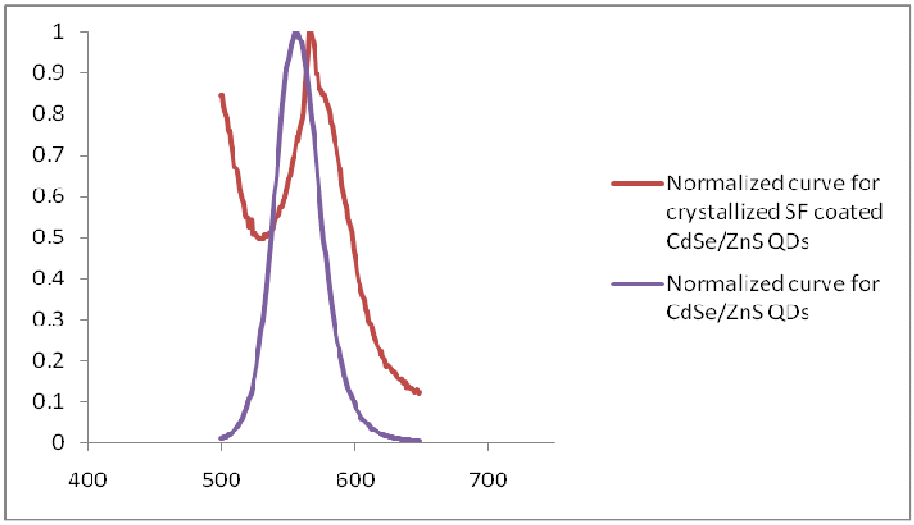

Figure 19. Normalized emission curve for crystallized SF coated QDs.

The curve demonstrates a slight red-shift for coated QDs. This result is consistent with earlier reports of red shift in QD emission as a result of coating by amphiphilic block copolymer[5] as SF is similar to an amphiphilic block copolymer.[85]

To verify the biocompatibility of SF coated QDs, HeyA8 cells were exposed to these particles. The cells were imaged using Zeiss Axiovert microscope at t=1 hr and t=12 hours post exposure respectively. Figures 20 (a) and (b) are representative of t=1 hr images of these cells. The QDs appear to have enodcytosed with apparent mitigation of the cyto-toxicity of uncoated dots. The lack of floating cells and floating luminescent particles demonstrate that the SF coated QDs had either entered the cells or had been washed away during the PBS washes.

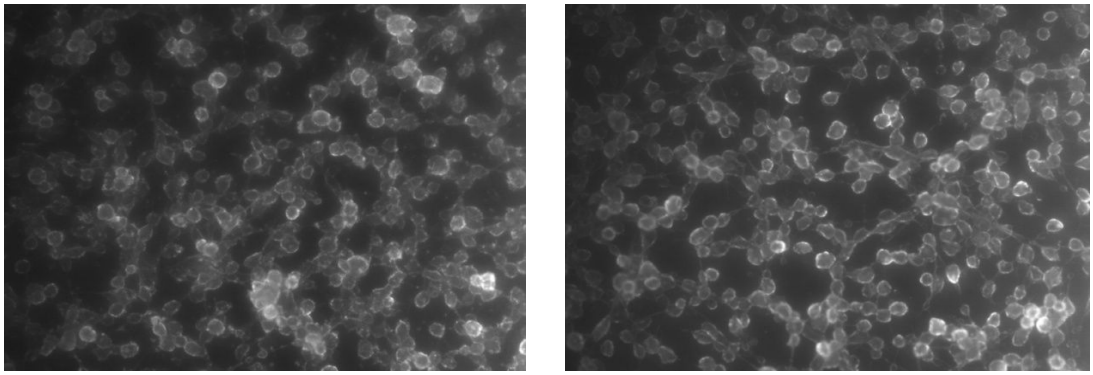

Figure 20. T=1 hour post exposure fluorescence images of HeyA8 cells exposed to SF coated QDs.

Figures 21 (a) and (b) correspond to t=12 hours post-exposure images taken from the same set of cells. Although the SF coated QDs display no apparent cytotoxicity, the cell membranes fluoresce more than the rest of the cell body indicative of colocalization of the dots in the plasma membrane. Steric hindrance was believed to be the cause of this

and an investigation of the TEM pictures, figure 22, for the sample used for this study confirmed this. The peak emission wavelength of these uncoated particles was 580 nm, corresponding to the size that the core was expected to be. However, since the overall size of the uncoated particle was approx 100 nm with appreciable polydispersity in the sample, it was concluded that we had a far thicker ZnS shell than necessary. The method of fabrication was modified to accommodate the necessary changes to decrease the size of the ZnS shell, the ZnS coating time was reduced from 60 minutes to 30 minutes resulting in a couple of monolayers of ZnS coating. The fluorescent image shows a more even distribution of SF coated QDs across the cell body once the ZnS shell was reduced to a thin layer.

As shown in figure 23, with a decreased thickness of ZnS shell, the SF coated QDs were more evenly distributed across the shell with relatively lesser colocalization in the plasma membrane of the cell. The concentration of cells used on each flask was $1x10^6$ cells. This is indicative of decreased steric hindrance, which can be attributed to a decreased overall particle size.

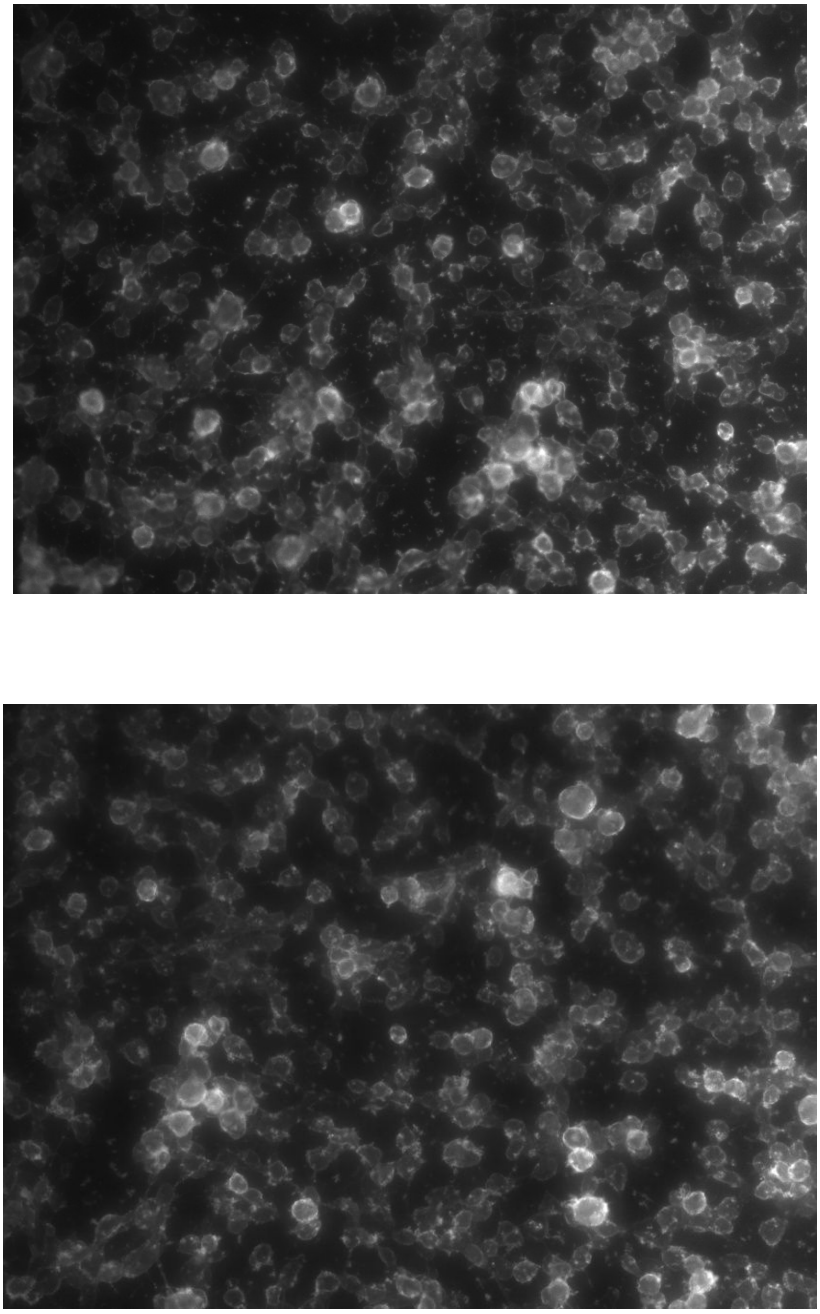

Figure 21. T=12 hour post exposure fluorescence image of HeyA8 cells exposed to SF coated QDs.

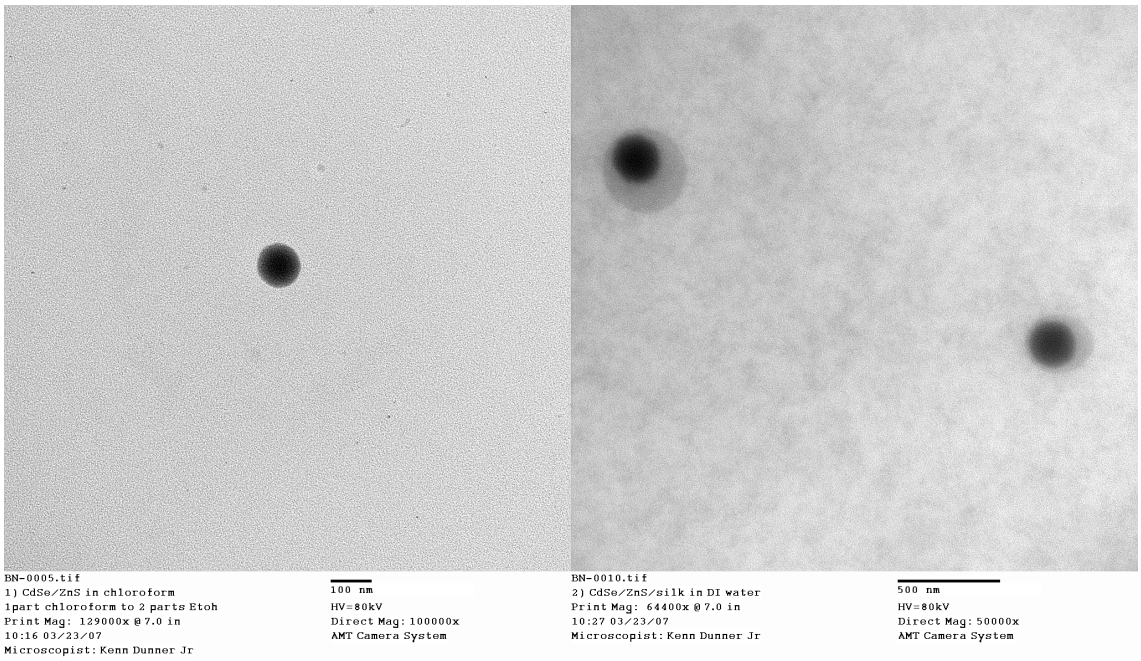

Figure 22. TEM images of uncoated and SF coated CdSe/ZnS QDs with a large (approx 50 nm) ZnS shell on the CdSe core.

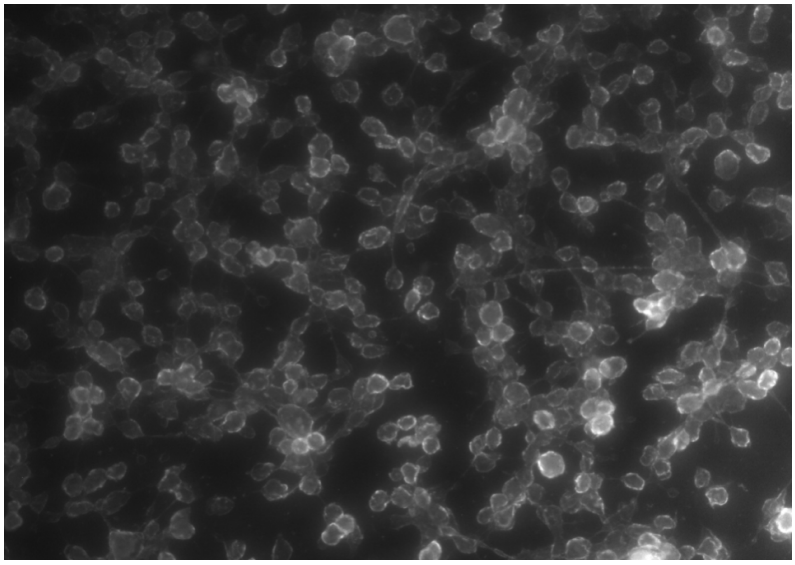

Figure 23. T=12 hour post exposure. HeyA8 cells exposed to SF coated CdSe/ZnS QDs.

To quantify the biocompatibility of SF coated QDs (610 nm peak emission wavelength) an MTT assay was carried out on HeyA8 ovarian cancer cells exposed to the SF coated QDs. The cell flask was trypsinized by adding 5 ml of trypsin to the flask. At 5 minutes, 5 ml of media was added to neutralize the trypsin and the cells were then collected in a 15 ml conical flask. The cells were the plated in the microtitter plate to a final concentration of $1x10^6$ cells/ml. After 24 hours of incubation at 37^0 C, media was removed from the wells. 100 ml of 10% MTT (3-(4,5-dimethylthiazol-2-yl)-2,5-diphenyltetrazolium bromide, a tetrazole) stock solution prepared in RPMI media was added per well. The plate was then incubated for 4 hours. 100 ml isopropanol was added to each well. The well contents were mixed using multiple pipetting cycles. The plate was placed on a "Flow" plate shaker for 20 min at low speed. At the end of 20 minutes, the plate was read using ELISA reader at 570 nm. The results of the assay are summarized in figure 24.

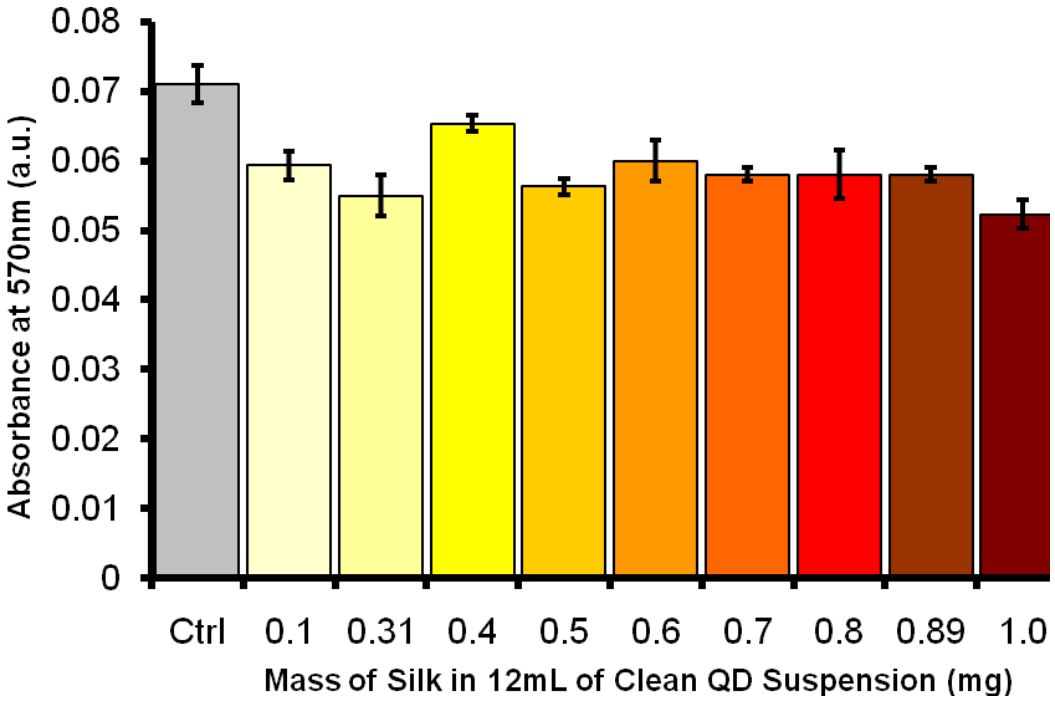

Figure 24. MTT assay of HeyA8 cells exposed to SF coated QDs.

The principle of MTT assay is the reduction of MTT to purple Formazan. This reduction occurs only in the presence of mitochondrial enzyme. Therefore, the amount of MTT reduction (Formazan formation) is dependent on the percentage of live cells in the well. This was quantified using the ELISA spectrophotometer. Cells not exposed to SF coated QDs were used as control. No significant difference ($P = 1.69 \times 10^{-7}$) was found between control and test cells. Furthermore, incremental amounts of SF was used during the coating process to get incremental coating thicknesses. However, the absorbance values for groups exposed to QDs with different thickness coatings also did not show significant difference. This was attributed to the fact that at 570 nm QDs would also absorb the incident light and hence would induce an error term in the absorbance

values. Therefore, we concluded that MTT was not an ideal candidate to perform a live/dead study on these cells.

As described, a two step conjugation process was carried out to conjugate SF coated QDs to streptavidin and phalloidin respectively. Schematics shwoing the resultant particles and their subsequent use for cellular labeling are shown in figures 25 and 26. As shown in figure 25 streptavidin was conjugated on the surface of SF coated QD, using conventional EDC chemistry. The same technique was used to conjugate phalloidin to SF coated QDs as shown in figure 26. Proteins on the surface of HeyA8 cells were non-specifically biotinylated using the piercenet biotinylation kit as described earlier. Biotinylated HeyA8 cells were incubated with streptavidin conjugated SF coated QD for 1 hour. Streptavidin has a very high affinity for Biotin and this results in high efficiency of coupling between the bio-conjugated dots and the surface proteins on HeyA8 cells.[86] After 1 hour of incubation the QD solution was aspirated; the cells were given PBS washes (3X) and were imaged using the Zeiss microscope. Figure 27 shows a representative cell with the cell surface proteins labeled by SF coated QDs. As can be seen the entire surface of the cell has been labeled indicating a high efficiency of streptavidin-biotin coupling.

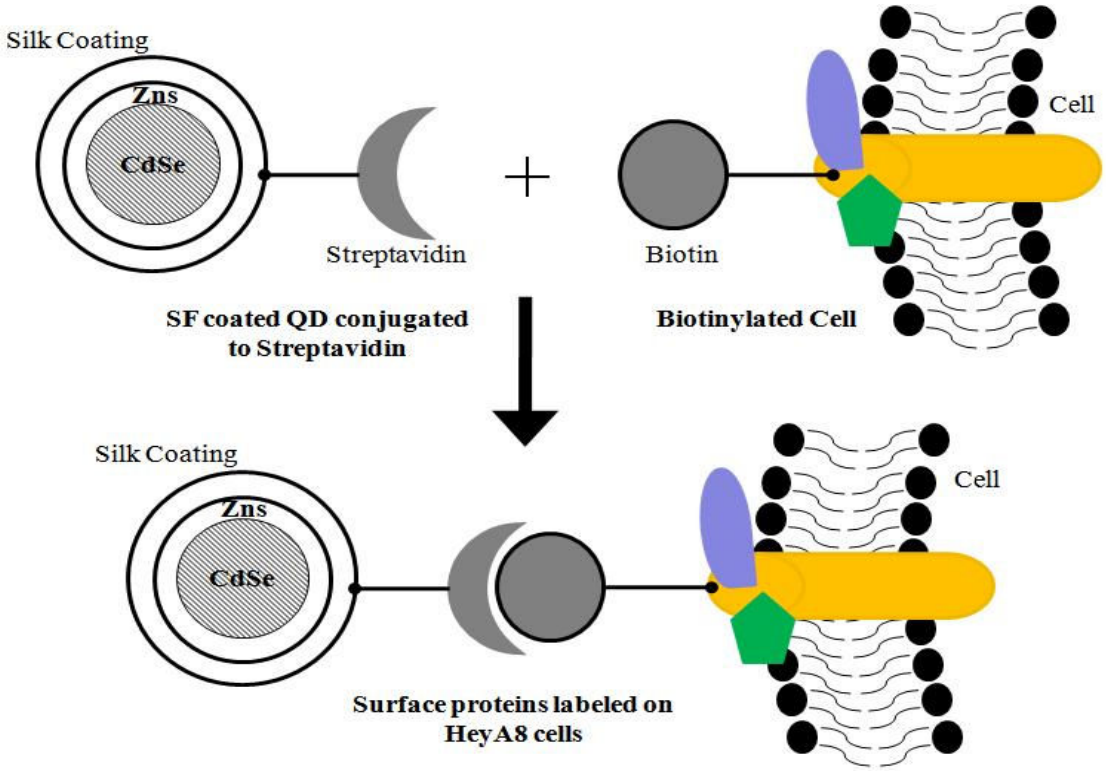

Figure 25. Schematic showing the 2 steps of labeling surface proteins on HeyA8 cells with streptavidin conjuagated SF coated QDs.

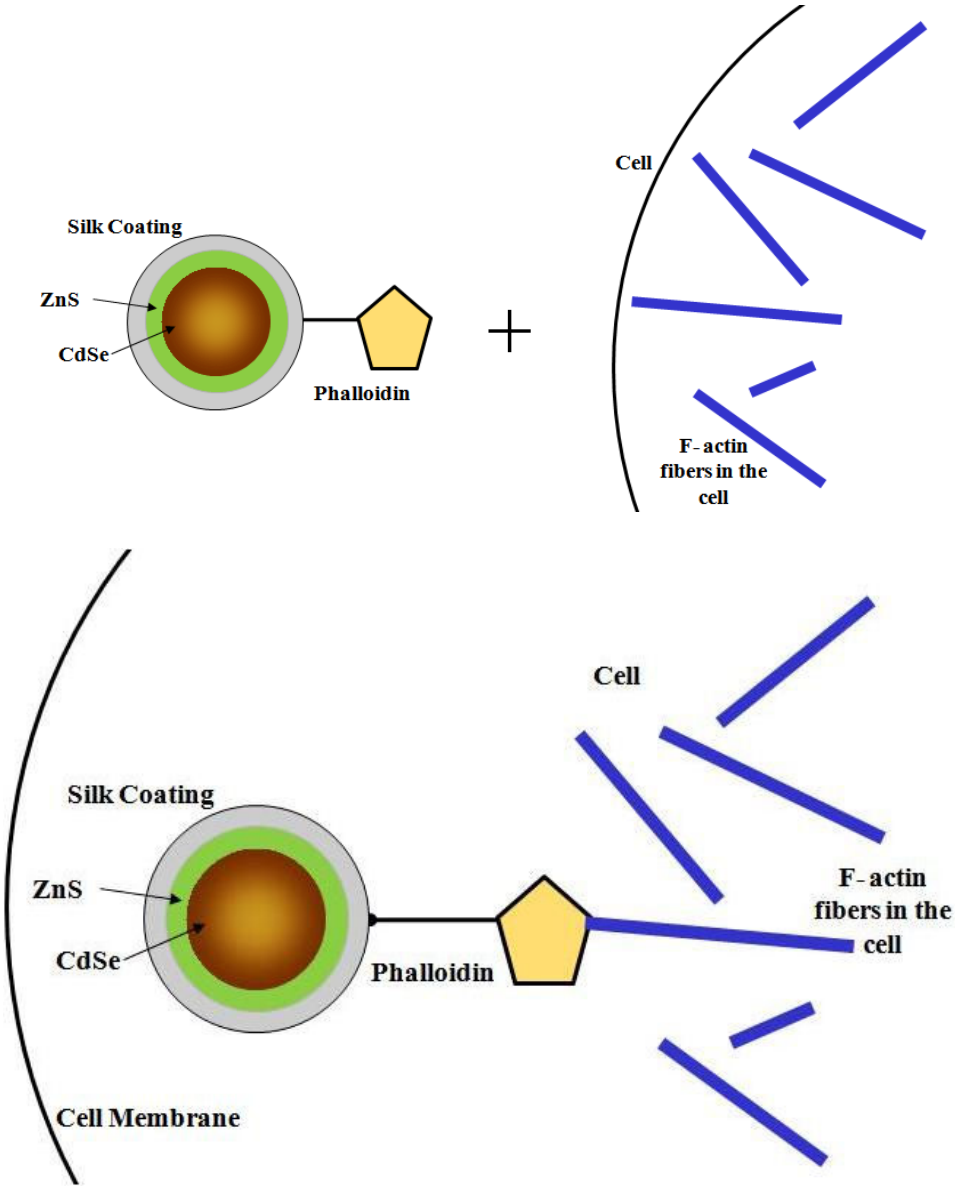

Figure 26. Schematic showing the 2 steps of labeling F-actin in HUVECS with phalloidin conjugated SF coated QDs.

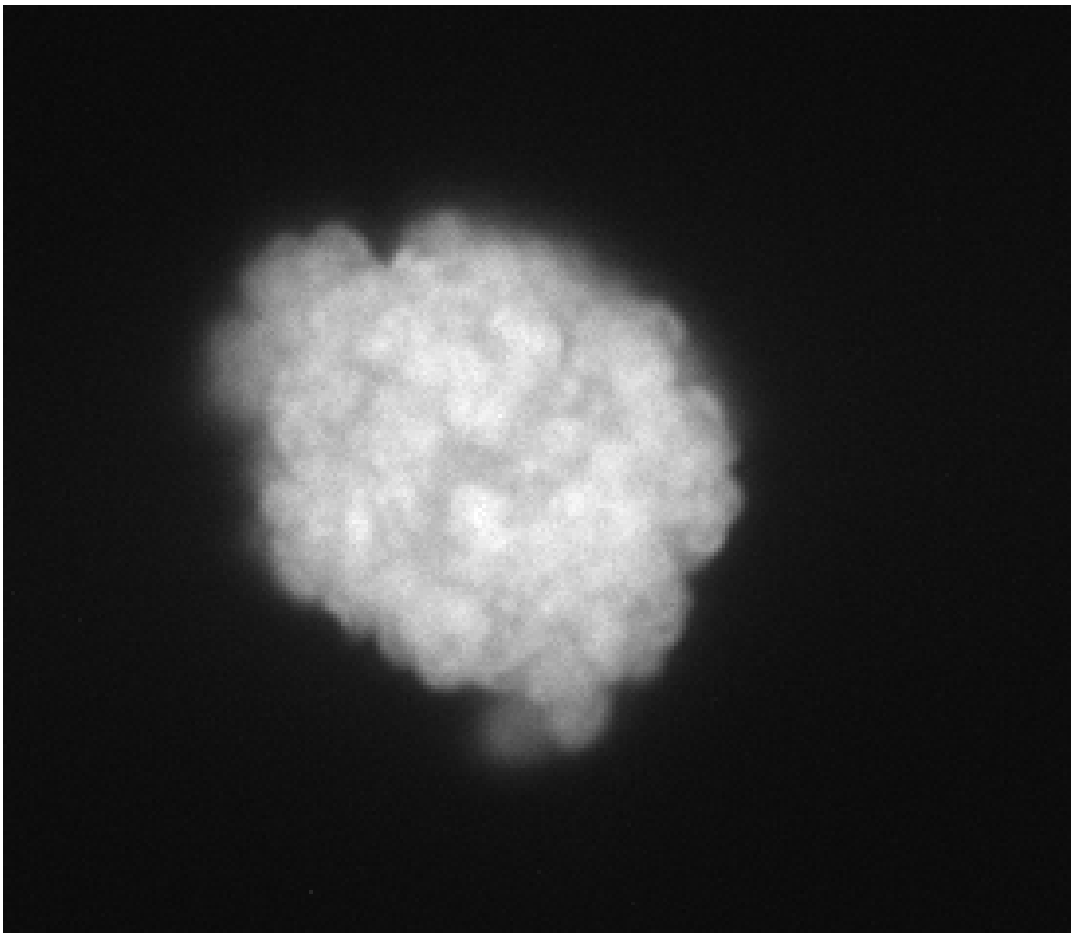

Figure 27. Figure representing surface protein labeling of HeyA8 cells by streptavidin conjugated SF coated QDs.

Figure 28 shows the labeling of F-actin on the cyto-skeleton of human umbilical vein endothelial cells (HUVECS). The cells were fixed and permeabilized as described in the methods section. The cells were then incubated with phalloidin conjugated SF coated QDs for 1 hour at room temperature. Like streptavidin/biotin, phalloidin has a very high affinity towards F actin[87]. Hence, phalloidin conjugated SF coated QDs label F actin on the fixed HUVECS with high efficiency. Figure 27 demonstrates labeling of F actin fibers. The contrast is indicative of high efficiency of coupling between phalloidin conjugated SF coated QDs and actin fibers.

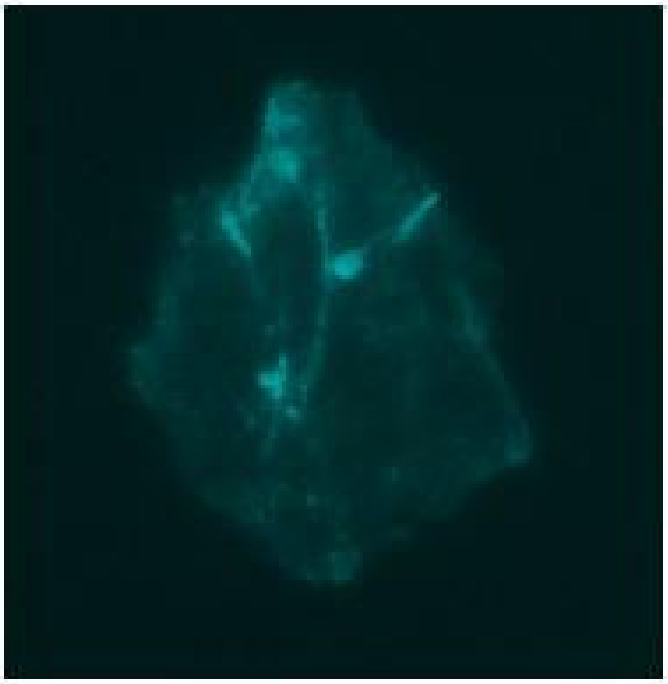

Figure 28. Labeling of F-actin in HUVECS using phalloidin conjugated SF coated QDs. The image has been false colored to enhance the contrast.

CHAPTER V

DISCUSSION, CONCLUSION AND FUTURE WORK

The experiments represent the first reported attempt to directly coat QDs with a naturally occurring protein. The technique reported here is significantly different from previously reported techniques.[2, 3, 88] The self assembled coating system described here can be used to coat different core-shell structures. Some of the potential applications for these types of quantum dot/protein conjugate systems include cell surface labeling and intra-cellular tracking, tumor labeling, and for a variety of other imaging applications.

The fabrication of CdSe/ZnS QDs was carried out using a one pot reaction method[7]. However, CdSe growth temperatures used were between 270^0 C and 300^0 C, whereas the temperature of ZnS growth was 200^0 C. The cooling time for the metallic bath was highly dependent on the ambient temperature and hence was a potential source of error in the prediction of QD peak emission wavelength. A second heating source may be used to reduce the error induced. A modified technique of fabricating CdSe cores, cleaning them and subsequently coating them with ZnS has previously been reported.[89]

For the silk fibroin coating of CdSe/ZnS quantum dots, 1,2,3, and 4 hour sonicated silk samples were used. No coating for the 1 hour sonicated silk was observed, whereas incrementally more particles were coated corresponding to 2,3, and 4 hour sonicated samples. The size of SF coatings were narrowly distributed. Variable size coatings may be required for in vivo labeling of different tissue regions. Therefore, a stoichiometry model corresponding to the SF coating chemistry needs to be developed in order to be used as a predictive tool to predict the coating thickness.

An obvious advantage of using this technique is that the robust structure of QDs fabricated using the organometallic synthesis is not altered before coating the QDs with SF. No ligand exchange occurs on the surface of the QDs and hence the chances of leaching of cadmium ions are reduced dramatically.

The mechanism of SF coating of QD is similar to that of QD encapsulation by an amphiphilic diblock or triblock copolymer. However, unlike the half-life profiles of synthetic polymer coatings reported earlier,[19, 20] studies have reported half-lives of SF coated nanoparticles to be much shorter.[90] Although a lot of variation has been reported in the literature depending upon the size of the particles, site of administration and the concentration of the SF coated particles,[91] the half-life typically ranges from a few hours to a few days. Additionally, the biocompatibility and protease susceptibility of SF have been demonstrated previously.[80] Therefore, it would be safe to speculate the candidacy of SF coated QDs for in vivo applications. An extensive study to quantify the half-life of SF coated QDs in vivo can be undertaken. Specific regions of interest such as the lymph nodes can been labeled and the luminescence observed over definite time intervals to quantify the half life of these QDs.

Unlike the technique reported earlier to achieve peptide coating of QDs using recombinant protein,[17] no charge labeling of protein was required in the author's case. Earlier studies have shown the use of protein coated QD assembly as sensor elements to sense cellular environmental properties such as pH.[17] Use of such particles as FRET sensors has also been reported.[92] Further work is being done at our lab to investigate the utility of SF coated QDs for pH measurements in the biologically relevant, slightly basic,

pH range. Also of interest to the lab is the application of QD coated particles as FRET donors.[93]

SF coated QDs were conjugated to phalloidin and streptavidin using EDC chemistry to endow specificity to the particles for use as labeling agent. Similar chemistry can be used to conjugate SF coated QDs to different anti-bodies and labeling proteins. This would lead to the use of SF coated QDs, for a variety of labeling applications, as luminescent nanoprobes.

This simple micellar self assembly system can also be used to coat other nanoparticle systems. The use of SF to coat liposomal particles for drug delivery has previously been reported.[33] The author speculates on the use of SF to coat different varieties of nanoparticles in a common system resulting in multi modal nanoparticles.[94]

We also showed the use of SF coated QDs to label focal adhesion complex proteins. The role of focal adhesion complexes and specific proteins participating in the formation of focal adhesion complexes such as integrins has been studied earlier in the process of tumor invasion.[95] The similarities between ECM degradation required for the spreading of metastatic tumor cells and that required for endothelial cells have also been studied.[96] Another line of investigation has been the role played by integrin alpha V beta III in tumor progression.[97] An antagonist to this molecule (vitaxin) is in phase II clinical trial as of the writing of this thesis.[98] The ability to visualize all the component proteins participating in the formation of focal adhesion complex would greatly enhance our ability to understand the dynamics at work governing the role played by FAC in tumor progression and potentially allow us to develop therapeutic interventions. This project is approachable now because of the ability of quantum dots to spectrally multiplex

information. SF coated QDs with different emission peaks can be all be excited simultaneously using a common high energy light source. This would enable the labeling of different components of the FAC using QDs emitting different colors and allow us to use a common light source for excitation. We could induce the formation of FAC using an AFM tip and study the FAC formation dynamics by following exciting the QDs using an evanescent field. Therefore, a combination of TIRF and AFM to image bio-conjugated SF coated QDs would provide an ideal platform to conduct such a study.

REFERENCES

(1) Dubertret, B.; David P.S.; Norris, J.; Noireaux, v.; Brivanlou, A.H.; Libchaber, A. *Science* **2002,** *298*, 1759-1762.

(2) Chan, W., Nie S. *Science* **1998,** *281*, 2016-2018.

(3) Bruchez, M.; Moronne M.; Gin, P.; Weiss, S.; Alivisatos, P. *Science* **1998,** *281*, 2013-2016.

(4) Stroh, M.; Zimmer J.; Duda, D.; Levchenko, T.; Cohen, K.; Brown, E.; Scadden, D.; Torchilin, V.; Bawendi, M.; Fukumura, D.; Jain, R. *Nature Medicine* **2005,** *11*, (6), 678-682.

(5) Wu, X.; Liu H.; Liu, J.; Haley, K.; Treadway, J.; Larson, J.P.; Ge, N.; Peale, F.; Bruchez, M.P. *Nature Biotechnology* **2003,** *21*, 41-46.

(6) Cai, W.; Shin D.; Chen, S.K.; Gheysens, O.; Cao, Q.; Wang, S.; Gambhir, S.S.; Chen, X. *Nano Letters* **2006,** *6*, (4), 669-676.

(7) Peng, Z.A.; Peng A. X. *J Am. Chem. Soc.* **2001**, *123*, 183-184.

(8) Smith, A.M.; Duan H.; Rhymer, M.; Ruan, G.; Nie, S. *Physical Chemistry Chemical Physics* **2006**, *8*, 3895-3903.

(9) Michalet, X.; Pinaud F.; Bentolila, L.A.; Tsay, J.M.; Doose, S.; Li, J.J.; Sundaresan, G.; Wu, A.M; Gambhir, S.S.; Weiss, S. *Science* **2005,** *307*, 538-544.

(10) Pathak, S.; Choi S.; Arnheim N.;, Thompson, M.E. *J. Am. Chem. Soc.* **2001,** *123*, 4103-4104.

(11) Kim, S.; Bawendi, M. G. *J. Am. Chem Soc*. **2003**; *125*, 14652-14653.

(12) Guo, W.; Li J.; Wang, Y.A.; Peng, X. *Chem. Mater.* **2003,** *15*, 3125-3133.

(13) Pinaud, F.; King D.; Moore, H.P.; Weiss, S. *J. Am. Chem. Soc.* **2004,** *126*, 6115-6124.

(14) Gao, X.; Warren C.; Nie, S. *Journal of Biomedical Optics* **2002,** *7*, (4), 532-537.

(15) Pellegrino, T.; Manna L.; Kudera, S.; Liedl, T.; Koktysh, D.; Rogach, A.; et al *Nano Letters* **2004,** *4*, (4), 703-707.

(16) Osaki, F.; Kanamori T.; Sando, S.; Sera, T.; Aoyama, Y. *J. Am. Chem. Soc.* **2004,** *126*, (21), 6520-6521.

(17) Mattoussi, H.; Mauro J.; Goldman, E.; Anderson, G.; Sundar, V., et al *Journal of American Chemcial Society* **2000,***122*, 12142-12150.

(18) Daniele, G.; Pinaud F.; Shara, W.; Wlfgang, P.; Daniela, Z.; Shimon, W. et al. *Journal of Physical Chemistry B* **2001,** *105*, (37), 8861-8871.

(19) Gao, X.; Yuanyuan C.; Levenson, R.; Chung, L.; Nie, S. *Nature Nanotechnology* **2004,** *22*, (8), 969-976.

(20) Ballou, B.; Lagerholn B.; Ernst, L.A; Bruchez, M.P.; Waggoner, A.S. *Bioconjugate Chemistry* **2004**, *15*, 79-86.

(21) Clapp, A.; Goldman E.; Mattoussi, H. *Nature Protocols* **2006,** *1*, 1258-1266.

(22) Reed, M. A. *Scientific American* **1993,** *268*, (1), 118-123.

(23) Ekimov, A.; Kriengol'd, F.; Kulinkin, B. *Soviet Physics - Semiconductors (English Translation)* **1989,** *23*, (9), 965-6.

(24) Murray, C.; Norris, D.; Bawendi M. *J. Am. Chem. Soc.* **1993,** *115*, 8706-8715.

(25) Yun, Z.; Zhengtao, D.; Jiachang, Y.; Fangqiong, T.; Qun, W. *Analytical Biochemistry* **2007,** *364*, (2), 122-127.

(26) Li, C.; Murase N. *Proceedings of SPIE* **2004,** *5361*, 150-157.

(27) Chen, M.; Gao, L. *Journal of the American Ceramic Society* **2005,** *88*, (6), 1643-1646.

(28) Datta, A.; Saha, A.; Sinha, A.; Battacharya, S.; Chatterjee, S. *Journal of Photochemistry and Photobiology B: Biology* **2005,** *78*, (1), 69-75.

(29) Dabbousi, B.; Rodriguez-Viejo, J.; Mikulec, F.; Heine, J.; Mattoussi, H.; Ober, V.; Jensen, K.; Bawendi, M. *J. Phys. Chem. B.* **1997,** *101*, (46), 9463-9475.

(30) Mansson, A.; Sundberg, M.; Balaz, M.; Bunk, R.; Nicholls, I.; Omling, P.; Tagerud, S.; Montelius, L. *Biochemical and Biophysical Research Communications* **2004,** *314*, (2), 529-534.

(31) Jaiswal, J.; Mattoussi, H.; Mauro, J.M.; Simon, S.M. *Nature Biotechnology* **2002,** *21*, 47-51.

(32) Dubertret, B.; Skourides, P.; Norris, D.J.; Noireaux, V.; Brivanlou, A.H.; Libchaber, A. *Science* **2002,** *298*, (5599), 1759-1762.

(33) Cheema, S.; Gobin, A.; Rhea, R.; Lopez-Berestein, G.; Newman, R.A.; Mathur, A.B. *Pharmaceutical Nanotechnology* **2007**, *341*, 221-229.

(34) Jin, H.; Chen, J.; Karageorgiou, V.; Altman, G.H.; Kaplan, D.L. *Biomaterials* **2004,** *25*, 1039-1047.

(35) Santin, M.; Motta, A.; Freddi, G.; Cannas, G. *J. Biomed Mater Res* **1999,** *46*, 382-389.

(36) Demura, M.; Minami, M.; Asakura, T.; Cross, T.A. *J. Am. Chem. Soc.* **1998,** *120*, 1300-1308.

(37) Howe, A.; Aplin, A.; Alahari, S.K.; Juliano, R. *Current Opinion in Cell Biology* **1998,** *10*, (2), 220-231.

(38) Lukashev, M.; Werb, Z. *Trends in Cell Biology* **1998,** *8*, (11), 437-441.

(39) Mizejewski, G. *Proceedings of the Society for Experimental Biology and Medicine* **1999,** *222*, 124-138.

(40) Turner S.; Sherratt, J. *Journal of Theoretical Biology* **2002,** *216*, (1), 85-100.

(41) Sasisekharan, R.; Shriver, Z.; Venkataraman, G.; Narayanasami, U. *Nature Reviews Cancer* **2002,** *2*, 521-528.

(42) Alberts, B.; Johnson, A.; Lewis, J.; Raff, M.; Roberts, K.; Walter. P. *Molecular Biology of the Cell* **2008,** *4*, 1071-1083.

(43) Chen, C.; Alonso, J.; Ostuni, E.; Whitesides, G.; Ingber, D.E. *Biochemical and Biophysical Research Communications* **2003,** *307*, (2), 355-361.

(44) Zameer, E.; Geiger, B. *Journal of Cell Science* **2001,** *114*, 3583-3590.

(45) Zaldel-Bar, R.; Cohen, M.; Addadi, L.; Geiger, B. *Biochemical Society Transactions* **2004,** *32*, (3), 416-420.

(46) Zimmerman, P.; David, G. *The FASEB journal* **1999,** *13*, S91-S100.

(47) Woods, A.; Couchman, J. *Trends in Cell Biology* **1998,** *8*, (5), 189-192.

(48) Couchman, J.; Woods, A. *Journal of Cellular Biochemistry* **1995,** *61*, (4), 578-584.

(49) Nikolovski, J.; Mooney, D. *Biomaterials* **2000,** *21*, (20), 2025-2032.

(50) Bloemen, P.; Henricks, J.; Bloois, L.; Tweel, M.; Bloem, A.C.; Nijkamp, F.P.; Crommelin, F.P; Storm, G. *FEBS Letters* **1995,** *357*, (2), 140-144.

(51) Stephens, D.; Allan, V. J. *Science* **2003,** *300*, 82-86.

(52) Axelrod, D. *J. Cell Biol.* **1981,** *89*, 141-145.

(53) Sund, S.; Axelrod, D. *Biophysics. J.* **2000**; *79*, 1655-1669.

(54) Sako, Y.; Minoguchi, S.; Yanagida, T. *Nature Cell Biology* **2000,** *2*, 168-172.

(55) Kuhn, J.; Pollard, T. *Biophys. J.* **2005,** *88*, (2), 1387-1402.

(56) Weiss, R.; Balakrishna, K.; Smith, B.A.; McConnell, H.M. *The Journal of Biological Chemistry* **1982,** *257*, (11), 6440-6445.

(57) Lang, T.; Wacker, I.; Wunderlich, I.; Rohrbach, A.; Giese, G.; Soldati, T.; Almers, W. *Biophysical Journal* **2000,** *78*, (6), 2863-2877.

(58) Vale, R.; Funatsu, A.; Pierce, D.; Romberg, L.; Harada, Y.; Yanagida, T. *Nature* **1996,** *380*, 451-453.

(59) Dickson, R.; Norris, D.; Tzeng, T.; Moerner, W.E. *Science* **1996,** *274*, (5289), 966-969.

(60) Ha, T.; Ting, A.; Liang, J.; Caldwell, W.B.; Deniz, A.; Chemla, D.D.; Schultz, P.G.; Weiss, S. *Proc. Natl. Acad. Sc.* **1999,** *96*, (3), 893-898.

(61) Han, W.; Ng, Y.; Axelrod, D.; Levitan, E.S. *Proc. Natl Acad Sci* **1999,** *96,* (25), 14577-14582.

(62) Rohrbach, A. *Biophys. J.* **2000,** *78*, (5), 2641-2654.

(63) Lagerholm, B.; Starr, T.; Volovyk, Z.N.; Thompson, N.L. *Biochemistry* **2000,** *39*, (8), 2042-2051.

(64) Sund, S.; Swanson, J.; Axelrod, D. *Biophys. J.* **1999,** *77*, (4), 2266-2283.

(65) Mathur, A.; Truskey, G.; Reichert, W. M. *Biophycal J.* **2000**; *78*, 1725-1735.

(66) Wang, M.; Axelrod, D. *Developmental Dynamics* **2005,** *20*, (1), 29-40.

(67) Omann, G.; Axelrod, D. *Biophysical Journal* **1996,** *71*, (5), 2885-2891.

(68) Bining, G.; Quate, C.; Gerber, C. *Physical Review Letters* **1986,** *56*, (9), 930-936.

(69) Alessandrini, A.; Facci, P. *Measurement Science and Technology* **2005,** *16*, R65-R92.

(70) Matzke, R.; Jacobson, K.; Radmacher, M. *Nature Cell Biology* **2001,** *3*, 607-610.

(71) Raab, A.; Han, W.; Badt, D.; Smith-Gill, S.J.; Lindsay, S.M.; Schindler, H.; Hinterdorfer, P. *Nature Biotechnology* **1999,** *17*, 901-905.

(72) Rotsch, C.; Radmacher, M. *Biophycal J*. **2000**; *78*, 520-535.

(73) Trache, A.; Trzekiakowski, J.; Gardiner, L.; Sun, Z.; Muthuchamy, M.; Guo, M.; Yuan, S.; Meininger, G.A. *Biophys J* **2005,** *89*, 2888-2898.

(74) Krautbauer, R.; Rief, M.; Gaub, H. E. *Nanoletters* **2003**; *3*, 493-496.

(75) Muller, D.; Baumeister, W.; Engel, A. *Proc. Natl. Acad. Sci* **1999**; *96*, 13170-13174.

(76) Fisher, T.; Oberhauser, A. F.; Carrion-Vazquez, M.; Marszalek, P. E.; Fernandez, J. M. *Trends in Biochemical Sciences* **1999,** *24*, (10), 379-384.

(77) Goldmann, W. H.; Galneder, R.; Ludwig, M.; Xu, W.; Adamson, E. D.; Wang, N.; Ezzell, R. M. *Experimental Cell Research* **1998,** *239*, (2), 235-242.

(78) Trache, A.; Meininger, G. *Journal of Biomedical Optics* **2005,** *10*, (6), 64023-64040.

(79) Sarkar, A.; Robertson, R.; Fernandez, J.M. *PNAS* **2004,** *101*, (35), 12882-12886.

(80) Gobin, A.S.; Froude, V.; Mathur, A.B. *Journal of Biomedical Materials Research Part A* **2005,** *74A*, (3), 465-473.

(81) Graareck, Z.; Gergely, J. *Analytical Biochemistry* **1990,** *185*, (1), 131-135.

(82) Daniels, G. M.; Amara, S. G.; Susan, G. A. *Methods in Enzymology* **1998**; *296*, 307-318.

(83) Kortan, A.R.; Hull, R.; Opila, R.L.; Bawendi, M.G.; Steigerwald, M.L.; Carroll, P.J.; Brus, L.E. *J. Am. Chem. Soc.* **1990,** *112*, (4), 1327-1332.

(84) Dobb, M.G.; Fraser, R.; Macrae, T.P. *The Journal of Cell Biology* **1967,** *32*, 289-295.

(85) Chen, X.; Knight, D.; Shao, Z.; Vollrath, Z. *Polymer* **2001,** *42*, (25), 09969-09974.

(86) Weber, P.; Ohlendorf, D.; Wendoloski, J.J.; Salemme, F.R. *Science* **1989,** *243*, (4887), 85-88.

(87) Wieland, T.; Vries, J.; Schafer, A.; Faulstich, A. *FEBS Letters* **1975,** *54*, (1), 73-75.

(88) Mitchell, G.P.; Mirkin, C.; Letsinger, R. *J. Am. Chem. Soc.* **1999**, *121*, 8122-8123.

(89) Murray, C.B.; Kagan, C.; Bawendi, M.G. *Annual Review of Material Science* **2000,** *30*, 545-610.

(90) Zhang, Y.; Xia, Y.; Shen, W.; Mao, J.P.; MinZha, X.; Shirai, K.; Kiguchi, K. *Journal of Biomedical Materials Research Part B: Applied Biomaterials* **2006,** *79B*, (2), 275-283.

(91) Shammakhi, N; Ndreu, A.; Yang, Y.; Ylikauppila, Y.; Nikkola, L.; Hasirci, V. *The Journal of Craniofacial Surgery* **2007,** *18*, (1), 3-17.

(92) Sapsford, K.E.; Medintz, I.; Golden, J.P.; Deschamps, J.R.; Uyeda,H.; Mattoussi, H. *Langmuir* **2004**, *20*, 7720-7728.

(93) Meissner, K.E.; Sun, Z.; Nathwani, B.; Needham, C.; Beckham, R.; Everett, W.N.; Fan, X.; Cote, G.; Meininger, G.A. *Proceedings of SPIE* **2008,** *6863*, (02).

(94) Ferrari, M. *Nature Reviews Cancer* **2005,** *5*, (3), 161-171.

(95) Keshet, E.; Ben, S. *J. Clin. Invest.* **1999,** *104*, (11), 1497-1501.

(96) Liotta, L. A.; Steeg, P. S.; Stetler-Stevenson, W. G. *Cell* **1991,** *64*, (2), 327-336.

(97) Eliceiri, B. P.; Klemke, R.; Stromblad, S.; Cheresh, D. A. *The Journal of Cell Biology* **1998**; *140*, 1255-1263.

(98) Elicieri, B.; Cheresh, D. *J. Clin. Invest.* **1999,** *103*, (9), 1227-1230.

APPENDIX

Photon Technologies International

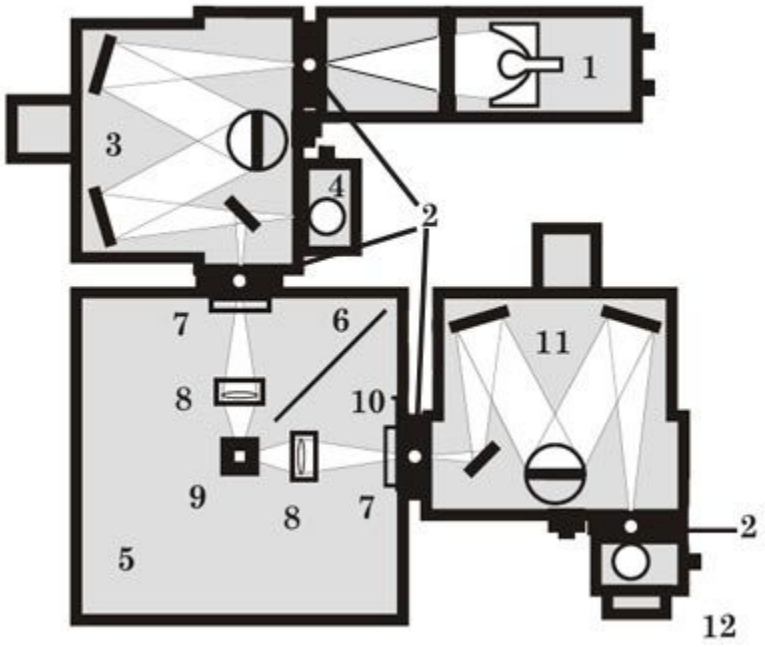

Figure A1. Top view of the Quantamaster Fluorometer used for this project.

Key to Figure

1 Flash lamp housing

2 Adjustable slits

3 Excitation monochromator

4 Excitation correction unit

5 Sample compartment

6 Baffle

7 Filter holders

8 Excitation/emission optics

9 Cuvette holder

10 Emission port shutter

11 Emission monochromator

12 Gated PMT detector

Dimension

(excluding computer and electronics)

System overall: 32 x 26 inches or 82 x 67 cm

Procedure for biotinylating proteins[71]

1. Remove the vial of Sulfo-NHS-Biotin from freezer and equilibrate it to room temperature before opening in Step 3.
2. Dissolve 1-10 mg protein in 0.5-2 ml of phosphate buffered saline (PBS) according to the calculation made.
3. Immediately before use, prepare a 10 mM Sulfo-NHS-Biotin solution by dissolving 2.2 mg in 500 micro liters of ultrapure water.
4. Add the appropriate volume of Sulfo-NHS-Biotin solution.
5. Incubatereaction on ice for two hours or at room temperature for 30-60 minutes.

VITA

Bhavik Nathwani was born at Jamnagar, on the west coast of the state of Gujarat, India on June 09, 1982. He attended St. Xavier's high school, through twelfth grade and entered Saurashtra University in 1999. He was awarded his B.E degree in Biomedical Engineering in 2003 and subsequently worked as a lecturer for the Biomedical Engineering Department at North Gujarat University from 2003 to 2005. His research interests include micro/nano technologies and their applications in Biomedical Engineering. After graduating in May 2008, Bhavik hopes to continue his education as a PhD student. He can be contacted at, 12 Ankur Apartment, Park Colony, Jamnagar, Gujarat, India – 361 008.